Archaeological and Anthropological Sciences (2024) 16:59
https://doi.org/10.1007/s12520-024-01962-1

RESEARCH

A multi-proxy geochemical and micromorphological study of the use of space and stratigraphy of a Viking-age house in Ribe, Denmark

Pernille L. K. Trant[1,2] · Barbora Wouters[2,4] · Sarah Croix[2] · Søren M. Sindbæk[2] · Pieterjan Deckers[3] · Søren M. Kristiansen[1,2]

Received: 13 August 2023 / Accepted: 3 March 2024 / Published online: 23 March 2024

Abstract
High-definition approaches are currently revolutionizing our understanding of the archaeology of urban archives. Multi-proxy studies at a high spatial resolution offer especially an opportunity to capture their high data potential. Here we present a study of complex floor layers from an occupation phase dating to c. AD 790–830 uncovered in the Viking-age emporium Ribe, Denmark (c. AD 700–900). In order to better understand stratigraphy and the use of indoor space, mapping for soil geochemistry (portable X-ray fluorescence analysis, pXRF) on a high-resolution grid (0.25 × 0.25 m, n = 1059), was combined with targeted sampling for soil micromorphology and artefact distributions. The results show that the studied occupation phase was composed of several short-lived floor phases belonging to two consecutive houses that had been sampled in conjunction, and which exhibited a complex stratigraphy. The older house phase had a primarily domestic function, where ten functional areas could be defined, and are interpreted as designated spaces for food preparation, storage, sitting or sleeping, and weaving. A younger house phase contained a metal workshop in addition to domestic functions. Methodologically, a number of new, potentially anthropogenic, elements of archaeological interest, such as arsenic, manganese and sulfur, were identified that may contribute to interpretations, while the multi-proxy approach elucidates the refined scale at which we can understand a complex stratigraphic sequence and the integrity of its units. This study shows how the various aspects of Viking-age urban life (craft production, domestic life) were integrated, and sheds light on the dynamics of urban occupation.

Keywords Viking-age house · Ribe · Geochemistry · Micromorphology · Artefact distributions · Stratigraphy · Use of space · Urban archaeology

Introduction

Complex urban stratigraphies offer many opportunities regarding the interpretative potential of sites. Thanks to their high level of detail, containing contextually sealed and oftentimes well-preserved remains, they can offer insights into the lives of urban societies in increasing resolution (Borderie et al. 2020; Croix et al. 2019a). Due to their complexity, they also present significant challenges during excavation. Changes in the urban fabric are oftentimes fast-paced, reflected as disturbances, truncations, constructions, or pits in the stratigraphy. In a number of cases, several meters of thinly-laid down stratigraphy can be discerned in Northwest European contexts (Croix et al. 2019a; Heimdahl 2005). However, sites in this climate zone present challenges related to their preservation conditions. These include the disappearance of organic matter due to intermittent drying from soil and groundwater table fluctuations, bioturbation by fauna and flora, or disturbances related to past or modern human activities (Borderie et al. 2020; Heimdahl 2005). All these factors render the focus on a single stratigraphic unit, for example, the occupation surface of a single house, increasingly difficult. In these cases, geoarchaeological

✉ Søren M. Kristiansen
smk@geo.au.dk

1 Department of Geoscience, Aarhus University, Aarhus, Denmark

2 Centre for Urban Network Evolutions, Aarhus University, Aarhus, Denmark

3 Archaeology, Katholieke Universiteit Leuven, Louvain, Belgium

4 Department of Art Science and Archaeology, Vrije Universiteit Brussel, Brussel, Belgium

methods are ideally suited to enhance the extent to which the depositional and post-depositional processes that shaped the archaeological record can be understood (Devos et al. 2020; Goldberg & Macphail 2006; Karkanas & Goldberg 2018; Macphail & Goldberg 2017; Mallol & Mentzer 2017; Matthews et al. 1997).

Ribe emerged as part of a small group of emporia around the North Sea from the end of the seventh century onwards including Dorestad, Quentovic, London, Southampton and York (Crabtree 2018; Loveluck 2013; Malbos 2017; Naylor 2016; Tys 2020). Later, the emporia network extended to Scandinavia with the foundation of Hedeby, Birka and Kaupang (Skre 2008; Feveile 2006a; Sindbæk, 2022b). These emporia acted as centres for exchange and cultural interactions linking Northern Europe to wider regions, eventually including the Mediterranean and Middle East (Ashby et al. 2015; Sindbæk, 2018; Sindbæk & Trakadas 2014). Remains from the earliest Ribe include occupation deposits that contain a large amount of artefacts, traces of crafts and organic remains (Croix et al. 2019a; Feveile 2006a). In 2017–2018, a research excavation on the site "Posthustorvet" took place to address a series of questions regarding the origin of the town around AD 700, the character of its earliest occupation, the nature of the thick, seemingly homogeneous strata on site ("dark earths" such as the so-called phase C, Feveile & Jensen 2000), and the dating of the town's youngest phases. As a result, the 2.3 m of complex, highly detailed stratigraphy were analysed in detail to understand the site's evolution through time.

The Northern Emporium Project's high-resolution research excavation has endeavoured to address some of the challenges faced in urban context (Sindbæk, 2018, 2022b). Current excavation techniques were combined with systematic stratigraphic recording by 3D-laser scanning, large-scale micromorphological sampling and geochemical analysis (Trant et al. 2020, 2021; Wouters 2018), the sieving of all excavated sediment, Bayesian modelling of high-resolution radiocarbon and dendrochronological dating (Philippsen et al. 2022) and detailed sampling for archaeological scientific analyses including zooarchaeology, archaeobotany, and entomology (Sindbæk, 2022a). Despite this multi-proxy strategy and a seemingly optimal preservation, it became increasingly clear that many units had been disturbed either during or after the site's existence. This was especially the case for strata from c. AD 750–760 onwards, where nearly no organic preservation remained. In order to grasp the formation and depositional history of one of the occupation phases dated to the period of c. AD 790–820, a detailed geoarchaeological and artefactual study was set up.

The design of this study involved mapping the use of space inside buildings (see for instance Cook et al. 2014; Crabtree et al. 2017; Croix 2015; Grabowski & Linderholm 2014; Macphail et al. 2016; Milek 2012; Milek et al. 2014; Rondelli et al. 2014; Smith et al. 2001; Sulas et al. 2019), and distinguishing indoor from outdoor spaces (e.g. Mikołajczyk & Milek 2016; Rondelli et al. 2014; Wilson et al. 2005). In the past, these types of research questions have been studied using the spatial distribution of macroscopically detectable artefacts or ecofacts (e.g. Croix 2020a), but increasingly also by applying geoarchaeological methods, such as geochemistry and soil and sediment micromorphology (e.g. Barrett et al. 2007; Grabowski & Linderholm 2014; Milek 2012; Milek & Roberts 2013; Milek & French 2007; Skre 2011), following the rationale that anthropogenic activities will leave traces on or in the sediment on which the activity took place. This might be either as chemical traces, or as relationships between components and disturbances that can be recognized on a microscopic scale (Mikołajczyk & Milek 2016; Sulas et al. 2019). Hence, the aims of this study are two-fold: 1) to disentangle a complex stratigraphy in this occupation phase, focusing on the most represented building and its depositional history; 2) despite the challenges posed by its stratigraphy, map the extent of the house and the different activity areas within it. These aims are achieved by the combined application of micromorphology with a dense geochemical analysis (X-ray fluorescence analysis (XRF) of elements, soil pH, and magnetic susceptibility), and artefact distributions based on high-resolution sampling. As part of this study, an overview of published literature on elements from indoor and outdoor activities is provided.

Study area

The study area, Ribe, is located in the southern part of Denmark (Fig. 1). Here, remains of a Viking-Age settlement were discovered in the 1970s (Bencard & Jørgensen 1990). Excavations between 1985 and 2000 demonstrated the potential of its intricate stratigraphy and provided significant progress in the understanding of site evolution (Feveile 2006a, 2006b). However, until 2017, excavations of early Ribe were limited to being either trenches or rescue excavations, sometimes executed on limited budgets (Sindbæk, 2018; 2022b).

Activities in Ribe were initiated around AD 700, and the town functioned as a centre for maritime trade and exchange of goods as well as cultural interaction before and throughout at least the first half of the Viking Age (c. 800–1050 AD, Ashby et al. 2015; Feveile 2012; Sindbæk, 2015; Sode et al. 2010). Ribe had a high settlement density and was situated on the banks of the river Ribe Å, providing a suitable river port approximately 5 km from the present-day coast (Ashby et al. 2015; Feveile 2012; Sindbæk, 2018). The traces of early Ribe include burials, fortifications, buildings, workshops and roads spread across a large area (Croix 2020b; Feveile 2006a, 2006b). The remains from Viking-age Ribe

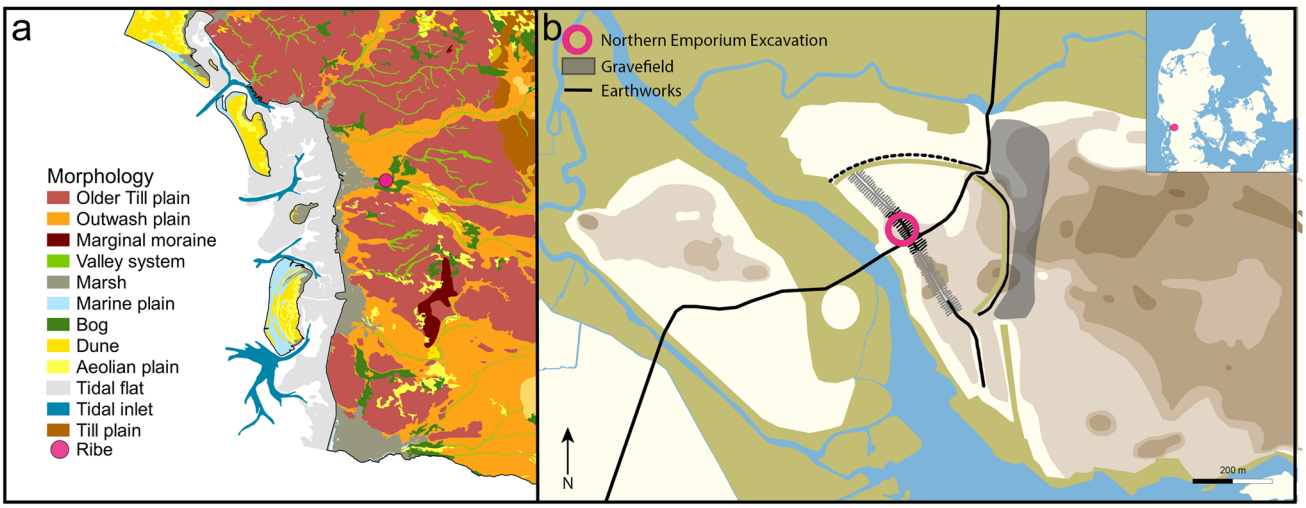

Fig. 1 **a**) Location of Ribe with the surrounding landscape. Data: Soil type map, GEUS. **b**) Reconstruction of Ribe in the Viking Age with the plot area from c. 700 AD onwards. The grave field was mainly in use in the eighth and ninth century, and the earthworks only appear after the middle of the ninth century. Graphics: Morten Søvsø and Louise Hilmar

are exceptionally well preserved in thick strata of occupation deposits containing a large amount of artefacts, wooden structures, waste from crafts and other remains (Bencard & Jørgensen 1990; Feveile 2006a; Sindbæk, 2018). The most widespread and well preserved remains are located north of Ribe Å (Sindbæk, 2015), containing traces of buildings and specialized activities on each side of a main street that divided the area into a system of plots laid out shortly after the beginning of activities (Feveile 2012; Søvsø 2020). Among documented activities are non-ferrous metalworking and iron work, glass bead production, amber working, bone and antler working, carpentry and textile production (Croix et al. 2019b; Feveile 2006b), which were either imported or locally produced (Barfod et al. 2022; Orfanou et al. 2021; Sode & Feveile 2002). Ribe was also centre for the first instances of coin-based trade in Scandinavia (Sindbæk, 2018; Feveile and Sindbæk, 2022).

The 2017 – 2018 Northern Emporium project excavated the full stratigraphy of a central part of the settlement area, including almost the full extent of one house plot (Plot 1), parts of the open areas surrounding the plot, the front part of the opposite plot (Plot 2) and a main street separating the plots (Sindbæk, 2018). The excavation was baptized "Posthustorvet" (between the former Post Office and the Art Museum, Sct Nicolaj Gade 10) within present-day Ribe and close to earlier excavations (see Feveile & Sindbæk, 2022a, b, Figs. 1 and 2).

On Plot 1, several distinctive clay floors were uncovered, and interpreted as representing different successive buildings and activity phases. These clay units appear to be related to the preparation, levelling or elevation during the re-building of (parts of) houses on top of older structures, or repairs of already existing floors. In the period from AD 760 onwards, such clay floors are systematically found on site, and present in most, but not all, parts of the houses. They are often overlain by thin, darker, sandy strata interpreted as the associated occupation deposits where activities took place. This sequence of clay-rich and sandy units provides useful information about the use of indoor space and activities in late-8th to early 9th-century Ribe.

Geoarchaeology and use of space

The implementation of geoarchaeological methods and techniques such as geochemistry and micromorphology can characterise past anthropogenic and natural processes that are not readily inferred using traditional archaeological methods.

Soil and sediment micromorphology has become frequently applied to urban sites during the past thirty years, and studies that focus specifically on house floors and urban use of space, within buildings as well as outdoors, have become more common (Banerjea 2018; Borderie et al. 2020; Crabtree et al. 2017; Gé et al., 1993; Karkanas and Van de Moortele 2014; Macphail & Goldberg 2017; Matthews 2005; Milek & French 2007; Milek 2005; Milek & Roberts 2013; Shahack-Gross et al. 2005; Shillito 2013, 2017). In addition, experimental and ethnographical research gains traction as one of the most important sources of knowledge regarding house floor formation, use of space and maintenance; building materials; and post-depositional processes (Banerjea et al. 2015; Lisá et al. 2020; Macphail et al. 2004; Milek 2012).

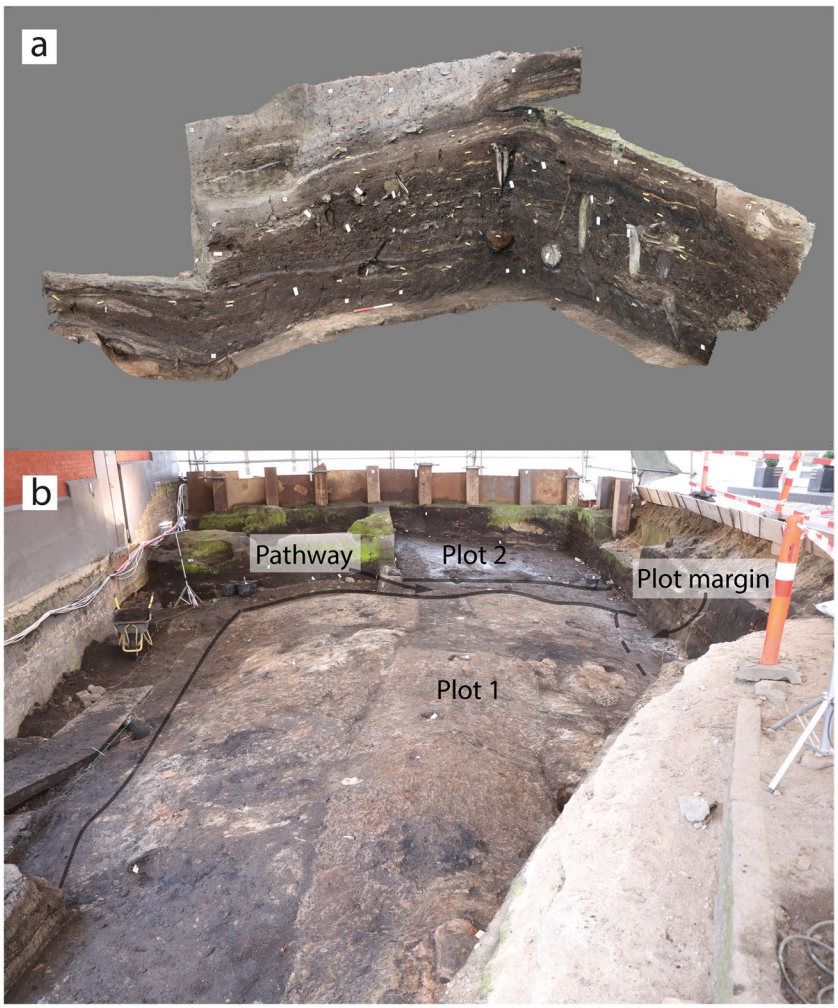

Fig. 2 **a**) Section of the best preserved part of the stratigraphy of the Viking-age emporium Ribe. **b**) The excavated areas used for this study (Plot 1, the pathway/street, and the plot margin). Plot 2 was not sampled for this study

Past site activities can be recognized as elemental signatures in the soil and, following analysis, as geochemical maps (Woodruff et al. 2009). Ethnographic case studies (e.g. Dore & Varela 2010; Rondelli et al. 2014) have shown conclusive evidence for the correlation between different domestic activities and elemental signal left in the sediment. Geochemical traces will represent either enrichments or depletions of the geochemical signal in the sediment (Mikołajczyk & Milek 2016; Sulas et al. 2019). Hence, geochemical signals will be recorded in the formed occupation deposits and as such may be recognized using various geochemical methods but undetectable by other methods.

Several studies have identified a range of elements that can be associated with different anthropogenic activities (Table 1). However, further work is still needed to fully understand the potential of soil and sediment geochemistry, and how these archives can be applied in archaeological contexts, as the presence of some elements is due to post-depositional processes, and is hence controlled by availability of the element, biological uptake, environmental conditions in the soil, and time (Parker & Toots 1970; Schulin et al. 2010; Tyler 2004).

Material and methods

A deposit on Plot 1 archaeologically interpreted as an indoor occupation surface was sampled to study the use of space using high-resolution multi-proxy geochemical analysis and micromorphology. The deposit was sampled for geochemistry in a dense grid (0.25 m × 0.25 m) and for micromorphology at strategically selected places (Trant et al. 2021). Additionally, large bulk sediment samples were collected from 0.5 m × 0.5 m grid squares for flotation and 1 mm wet sieving. The occupation phase was largely formed by stratigraphic unit A263, which belonged to the upper phase (phase c) of house K22. Due to indistinctiveness in the stratigraphy, a limited area belonging to the lowest phase of the house overlying K22c, K23, was also sampled (Fig. 3). This area, A264, contained a workshop for non-ferrous metalworking. Also, some areas

Table 1 Overview of elements recognised as markers for anthropogenic activities based on previous geoarchaeological studies, as well as associated geological affinities and behaviour, in temperate region soils

Element	Archaeological proxy for	Geological affinity	References
Ag	Use of marine resources, tanning, use of pigments and metal working	Adsorbes to especially organic matter (OM). Fe and Mn oxides can adsorb Ag-ions from solution. Can be mined as a byproduct of Ni, Pb and Zn deposits	Alloway 2013; Sulas et al. 2017
Al	Burning, cooking, metal-bearing resources (e.g. tanning/pigments), presence of metals, for correlation to background soil composition, depletion in floor layer	Clay particles. Smaller amounts associated with clay surfaces and soil OM. Forms part of hydroxides, adsorption to soil surfaces, complexation to OM and incorporated into plant tissue	Bohn et al. 2001; Fleisher & Sulas 2015; Oonk et al. 2009; Sulas et al. 2017
As		Aerobic: Concentrated in Fe-(oxy)hydroxides, also (oxy) hydroxides of Al and Mn, clay minerals and OM. Anaerobic: As sulfide minerals can precipitate	Alloway 2013
Au	Fragments, droplets, or enrichment from metalworking	May bond strongly to OM. Strong nugget effect	Alloway 2013; Wouters et al. 2017
Ba	Common anthropogenic marker, plant nutrient, marine foodstuff, household waste, middens, hearths, dung, areas with significant OM	Concentrated in Mn and P concretions and specific adsorbed onto oxides and hydroxides. Common element in the crust. Not very mobile in most soils	Alloway 2013; Entwistle & Abrahams 1997; Fleisher & Sulas 2015; Milek & Roberts 2013; Sulas et al. 2019; Wilson et al. 2005; et al. 2008
Ca	Common anthropogenic marker, plant nutrient, wood ash, seawater (together with Na and S in sea-related products or processes), foodstuff in general, marine foodstuff, household waste, middens, hearths, dung, areas with significant OM	Retention mainly determined by pH, then OM, clay minerals and oxides. High Ca (and Mg) indicates nearly neutral or higher pH as Ca replace protons on adsorption sites	Blume et al. 2015; Bohn et al. 2001; Mikołajczyk & Milek 2016; Milek & Roberts 2013; Sulas et al. 2017, 2019
Cr	Floor layers	Incorporated into Fe-hydroxides and strongly bound on Fe-oxides. Micronutrient	Oonk et al. 2009
Cu	Common anthropogenic marker, plant nutrient, use of sea-resources, tanning/use of pigments, household waste, metalworking, middens, hearths	High affinity for OM. Associated to clay surfaces and OM. Stable complexes with many organic and inorganic ligands (adsorption). Higher solubility at lower pH and lower amount of OM. Highly insoluble in reduced environments (precipitates as metal or very stable sulfides). Micronutrient	Alloway 2013; Bohn et al. 2001; Fleisher & Sulas 2015; Sulas et al. 2017, 2019; Wilson et al. 2008
Fe	Common anthropogenic marker, plant nutrient, foodstuff in general, household waste, middens, hearths, dung, enriched in OM deposits, burning, metalwork, depletion in floor layers	Smaller amounts associated with clay surfaces and SOM. Stable complexes with many organic and inorganic ligands (adsorption)—forms part of hydroxides, adsorption to soil surfaces, complexation to OM and incorporated into plant tissue. Micronutrient	Bohn et al. 2001; Cook et al. 2014; Mikołajczyk & Milek 2016; Oonk et al. 2009; Sulas et al. 2017, 2019
K	Common anthropogenic marker, plant nutrient, wood ash, seawater (together with Na and S in sea-related products or processes), foodstuff in general, marine foodstuff, household waste, middens, hearths	Moderately retained in soils with certain clay minerals (fits between their layers)	Bohn et al. 2001; Entwistle & Abrahams 1997; Milek & Roberts 2013; Sulas et al. 2017, 2019
Mg	Common anthropogenic marker, plant nutrient, seawater (together with Na and S in sea-related products or processes), salt, foodstuff in general, marine foodstuff, household waste, middens, hearths, metalworking, areas with significant OM content	See Ca	Milek & Roberts 2013; Sulas et al. 2017, 2019

Table 1 (continued)

Element	Archaeological proxy for	Geological affinity	References
Mn	Common anthropogenic marker, plant nutrient, animal herding (increased Mn and P), roofed spaces, marine foodstuff, household waste, middens, hearths, enriched in OM deposits, burning, metalworking	Mainly found as stains, curtains, nodules or concretions. Stable complexes with many organic and inorganic ligands (adsorption)—forms part of hydroxides, adsorption to soil surfaces, complexation to OM and incorporated into plant tissue. Associated to clay surfaces and OM. Often associated with Fe. Oxidised by microorganisms at pH > 4. Mn oxides are good at sorption of trace metals. Micronutrient	Alloway 2013; Bohn et al. 2001; Fleisher & Sulas 2015; Linderholm & Lundberg 1994; Mikołajczyk & Milek 2016; Sulas et al. 2017, 2019
Mo	Dung	Affinity for OM. High proportion of Mo in soils probably associated with OM and hydrated Fe-oxides	Alloway 2013; Sulas et al. 2019
P	Most widespread anthropogenic marker, plant nutrient, cooking, hearths, stabling, animal herding (Mn and P), roofed spaces, foodstuff in general, marine foodstuff, household waste, middens, dung, enriched in OM deposits, burning, metalworking	Strong interaction with many organic and inorganic soil components. Strong retention	Bohn et al. 2001; Cannell et al. 2020; Devos 2018; Mikołajczyk & Milek 2016; Milek & Roberts 2013; Nielsen & Kristiansen 2014; Sulas et al. 2017, 2019; Wilson et al. 2008
Pb	Burning, cooking, metal bearing resources, artefacts and household installations, roofed spaces, household waste, middens, hearths	Strong bonding to OM at pH > 4 in organic soils. Bonded to Fe-oxides in mineral soils. Stable complexes with many organic and inorganic ligands (adsorption). Fairly immobile, unless in very high concentrations	Alloway 2013; Cook et al. 2014; Fleisher & Sulas 2015; Macphail et al. 2016; Sulas et al. 2017, 2019; Wilson et al. 2005
S	Plant nutrient, seawater	Interacts with Ca^{2+}, Mg^{2+}, Al^{2+} and at positively charged sites on clay minerals. Biomass and SOM makes up large S reservoirs on the Earth's surface—especially in reduced soils and peatlands	Bohn et al. 2001; Cannell et al. 2020; Fleisher & Sulas 2015; Mikołajczyk & Milek 2016; Sulas et al. 2017; Zak et al. 2021
Si	Can likely dilute anthropogenic signals in datasets with variable and high quartz contents	Especially as a soil matrix as quartzitic sand and silt particles. Forms part of hydroxides, adsorption to soil surfaces, complexation to OM and incorporated into plant tissue (phytoliths). Largest component of non-carbonate soil. Sand fraction in soil usually > 85% quartz. Heavily weathered tropical soils down to 20% Si. Secondary Si formed as clay minerals after intensive weathering	Bern 2009; Blume et al. 2015; Bohn et al. 2001
Sn	Metalworking	Adsorption of inorganic Sn correlates to pH, OM content and CEC	Alloway 2013
Sr	Common anthropogenic marker, tanning and use of pigments, foodstuff in general, household waste, middens, hearths, enriched in seawater, areas with significant OM content, trace element in water, bones (meat preparation)	Retention mainly determined by pH, then OM, clay minerals and oxides	Blume et al. 2015; Cook et al. 2014; Fleisher & Sulas 2015; Mikołajczyk & Milek 2016; Milek & Roberts 2013; Sulas et al. 2017, 2019; Wilson et al. 2008
Zn	Common anthropogenic marker, plant nutrient, cooking, household waste, middens, hearths, dung, areas with significant OM content, metalworking	At high concentrations sorbed to clay minerals. Small amounts associated with clay surfaces and OM. Sorbed specific as Zn^{2+} onto pH-dependent oxyhydroxides and OM. Stable complexes with many organic and inorganic ligands. Micronutrient	Alloway 2013; Bohn et al. 2001; Cook et al. 2014; Fleisher & Sulas 2015; Milek & Roberts 2013; Sulas et al. 2017, 2019; Wilson et al. 2005, 2008

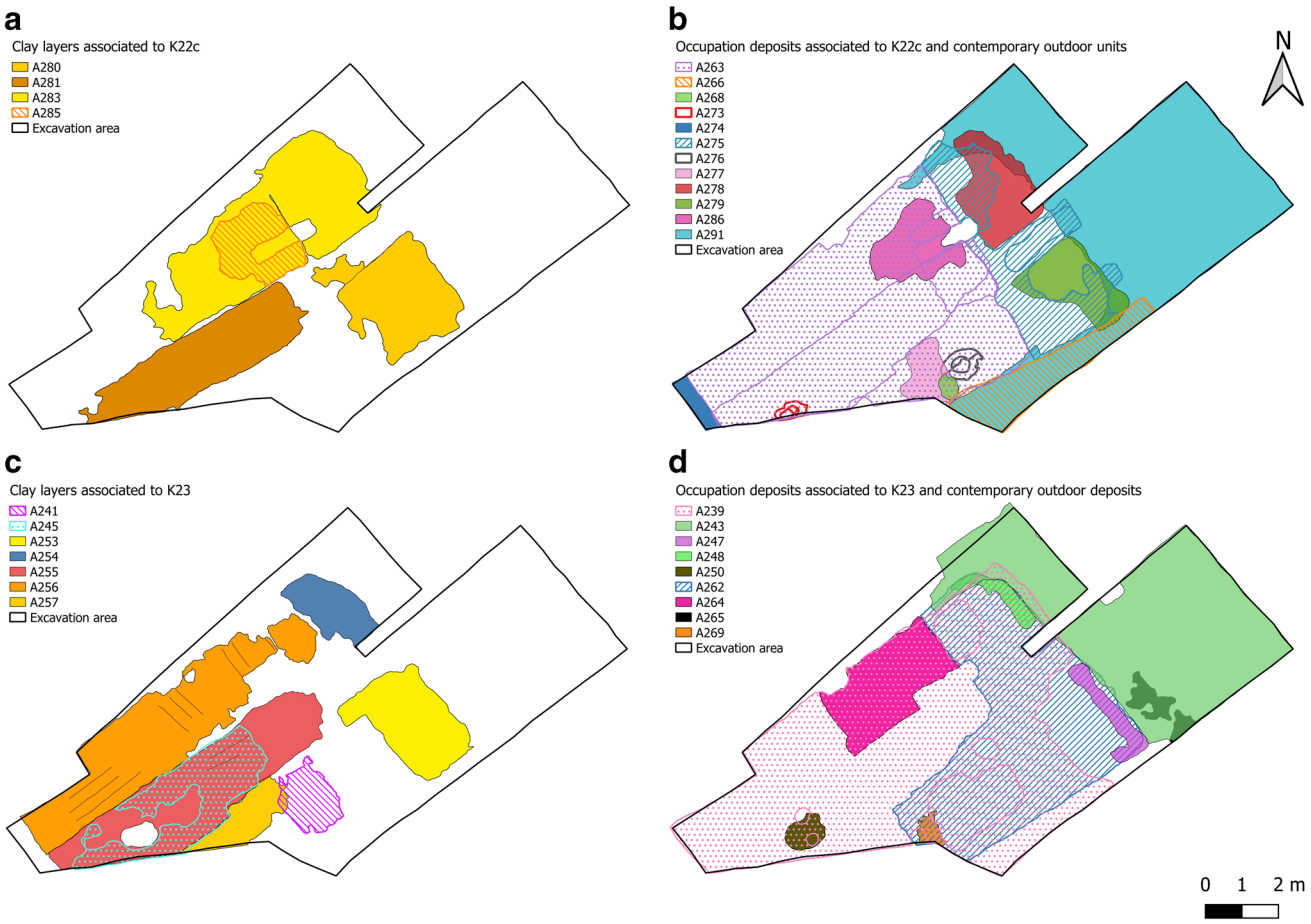

Fig. 3 Layout of clay layers and stratigraphic units. **a**) Clay layers associated to K22c. **b**) Occupation deposits associated to K22c and contemporary outdoor units. **c**) Clay layers associated to K23. **d**) Occupation deposits associated to K23 and contemporary outdoor units

without clay floors could not be strictly separated between K23 and K22c, with materials possibly representing both phases of occupation (A262). Difficulties in separating the clay floors arose due to subsidence, consolidation and deformation of the stratigraphy because of underlying features rich in organic matter. The sampled surface measured approximately 7 × 10 m and is radiocarbon dated to the period 780–820 AD (Philippsen et al. 2022).

During the excavation, it was possible to recognize a central aisle, two side aisles and two front rooms based on differences in sediment texture and colour, forming fairly similar floor plans in both K22c and K23. The outline of house K22c was defined by contiguous clay floors (contexts A280-A283), covered by different activity layers rich in sand and ash (among other parts of A262, A263 and A275). The occupation deposits appeared as thin, dark brown layers with a thickness varying from a few mm to a couple of cm, located directly on top of the clay floors. Additionally, a hearth (A273) and a collapsed baking oven (A276) were recognised. Of these units, only occupation deposits A262 and A263, hearth A273, and baking oven A276 were sampled for geochemistry, whereas most units in K22c and K23 are represented in the micromorphological block samples.

At the time of sampling, some units belonging to the younger house K23 were yet to be fully excavated and defined (A264 and parts of A262) and were thus included in the sampling. House K23 consisted of a sequence of layers containing among others clay floors, on top of which formed two activity layers, and a hearth. On site, A264 was recognized as a sharply defined, homogeneous, dark brown, charcoal-rich occupation deposit containing remains of non-ferrous metalworking.

Apart from the indoor layers, the sampling also covered an outdoor area (A266) south of Plot 1 interpreted on site as an open area between plots, which contained large amounts of animal bones in a dark homogeneous matrix, and part of the pathway/street (A243), which was observed as dark sediment with a localised, larger light patch of sand (A265). A265 marks the interface between A243 and the underlying street level A291, which both formed by continuous accumulation of similar materials. Thus, although A243 was the stratigraphic

unit sampled for geochemistry, the sampling likely included materials from the upper part of A291 as well.

Sampling and sample preparation

Bulk sediment sampling

A total of 1059 bulk sediment samples were collected from house phases K22c and K23 in a 0.25 m grid (Fig. 4a). The grid was laid out according to a 0.5 m grid fixed on an artificial horizontal surface. A Trimble SX10 (DGPS) high-density 3D laser scanning total station was used to record sub-cm precise coordinates of each sample and all samples were numbered according to the grid. Approximately 150 g sediment was collected within a radius of 10 cm around each grid point, and care was taken not to include any underlying layers. All samples were collected by the same persons over three days to minimize sampling and sampler bias.

All 1059 samples were air-dried at a approximately 27 °C, gently mortared and 2 mm sieved. Approximately 30 ml of each sample < 2 mm was representatively subsampled, ground with a Retsch RS200 to ensure homogeneity, and stored in medicine glasses.

Block sampling

Twenty-four undisturbed oriented blocks were analysed. They were collected from Plot 1 (Fig. 4c) by creating small vertical sections from which each individual block was collected, including the surface sediment sampled for geochemical analysis. The sample locations were selected according to the rationale of block sampling in complex, urban excavations (Wouters et al. 2016; Wouters 2018) and followed a number of main axes through the house, as well as particular locations where the original sediment might be better preserved, such as in corners, close to potential (internal) walls, etc., as well as a number of outdoor deposits surrounding the house (Fig. 4c). Prior to the block sampling, field descriptions were made according to the "Comprehensive Field Data Bases" (Langohr 1994) and the "Guidelines for soil profile description" (F.A.O., 2006; Table 2).

The air-dried undisturbed blocks were impregnated with resin and manufactured into thin sections (5 × 8 cm; thickness ~ 30 µm) by the Laboratory for Mineralogy and Petrography, Ghent University, according to the guidelines by Benyarku & Stoops (2005).

Geochemical analyses: Laboratory and spatial analyses

Multi-element analysis

All ground samples (Fig. 4a) were analysed for multi-elements in the laboratory using a Bruker S1 Titan 800 portable XRF scanner in a standardized setup. The pXRF includes an Rh anode tube with a maximum voltage of 50 kV/39 µA and the instrument works with a collimation standard of 5 mm and a five-position motorized filter changer. Before the main analysis, a reference sample with known elemental values was measured several times to choose the most suitable application and phase settings with shortest exposure times. Based on this, the chosen application was the mining mode "GeoChem" with "GeoChem General" settings, which includes full support for light elements through dual phase measurements. The phase settings were set to 30 s for both the first and second phase. A reference sample (NIST SRM 2702) was measured between samples to account for possible drifting in the instrument. All samples were measured in triplicates, with the resulting mean used as the element concentration (see details in Trant et al. 2021).

A total of 104 samples (approximately 10% of the full dataset, Fig. 4b) were randomly selected for multi-element analysis with inductively coupled plasma mass spectrometry (ICP-MS), providing in total 37 different elements. The ICP-MS analysis was performed with aqua regia extraction of the ground samples. The analysis was performed at Bureau Veritas, Canada. The accuracy of the dataset was validated by including both internal as well as international soil standards in the analysed batches. Lastly, the reliability of the measured concentrations were evaluated using Pearson correlation from 13 duplicate samples (all presented elements have $R^2 > 0.95$). On one impregnated block micro X-ray fluorescence (µXRF) elemental mapping was used to analyze the compositions of suspect small metal working residues using a Bruker Tornado M1 instrument and software.

Magnetic susceptibility

Magnetic susceptibility (MS) was measured using a Bartington MS3 magnetic susceptibility meter with a Bartington MS2B sensor. Magnetic susceptibility was measured on 278 samples, representing a 0.5 m grid (Fig. 4a) across the sampled surface. A priori it was not anticipated to be necessary with the very high resolution resulting from the 1059 samples constituting the 0.25 m grid (Fig. 4a) for analysis of MS. As a result, this lower resolution (0.5 m grid) was chosen for MS analysis.

Soil pH analysis

Soil pH was performed on 73 samples in the laboratory, representing a 1.0 m grid (Fig. 4a) using a MeterLab PHM240 pH/ion meter and a standard glass/calomel electrode. pH measurements were conducted following

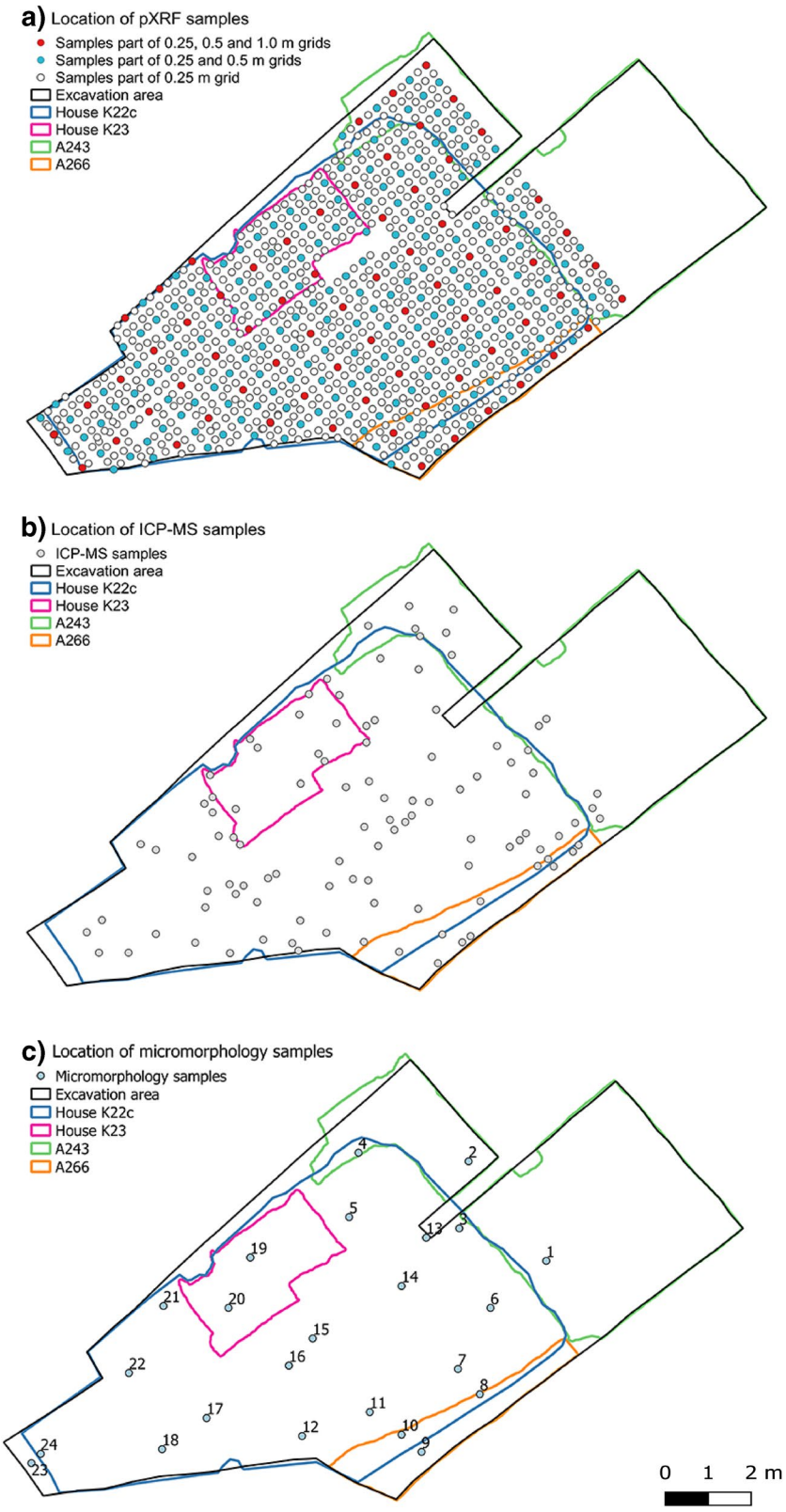

Fig. 4 Locations of block samples for micromorphology and multi-element analyses. **a**) The 0.25 m grid applied for bulk sampling to soil geochemistry and artefact distribution. Samples shown with red constitute parts of all three (0.25 m, 0.5 m and 1.0 m) grids deduced from the sampling grid, samples marked with blue are part of both the 0.5 and 0.25 m grid and samples marked with white are only part of the 0.25 m grid. **b**) Bulk soil samples randomly selected for ICP-MS analysis. **c**) Micromorphology samples

Table 2 Elemental values and statistics for concentrations measured with pXRF, magnetic susceptibility and soil pH

	N†	Min	Max	Range	Mean	Standard deviation	LOD‡
Ag	336	0.00027	0.218	0.218	0.0156	0.030	0.001
As	767	0.0013	0.00967	0.00837	0.00242	0.0009	0.0003
Ba	898	0.0263	0.0791	0.0528	0.0395	0.0066	0.019
CaO	1059	0.742	13.1	12.2	3.59	1.27	0.00518
Cl	451	0.0244	0.216	0.191	0.0336	0.0121	0.0135
Cu	1059	0.00155	1.12	1.11	0.0419	0.0684	0.0005
Fe_2O_3	1059	0.598	14.0	13.4	3.65	1.520	0.0013
K_2O	1059	0.626	2.18	1.55	1.14	0.187	0.005
MgO	229	1.36	2.43	1.06	1.78	0.209	1.027
MnO	1059	0.0355	4.13	4.10	0.369	0.330	0.002
Na	104	0.023	0.303	0.280	0.097	0.043	*
P_2O_5	1059	0.840	9.82	8.98	3.69	1.16	0.021
Pb	873	0.0018	1.22	1.22	0.0121	0.0501	0.001
S	562	0.0187	0.227	0.208	0.0591	0.0376	0.008
SiO_2	1059	22.6	85.5	62.9	59.9	7.39	0.107
Sn	638	0.0110	3.55	3.54	0.0992	0.305	0.002
Sr	1059	0.0071	0.0585	0.0514	0.0257	0.0063	0.0004
Zn	1017	0.0013	0.208	0.207	0.0180	0.0156	0.0003
Magnetic susceptibility	278	9.48	482	472	71.9	67.3	
pH	73	5.84	7.51	1.68	6.67	0.38	

†*Number of samples with concentrations above the limit of detection. Range, mean and standard deviation (SD) calculated based on all detected concentrations in percentage. Some elements were not detectable in all 1059 samples, giving different N for the dataset. All element concentrations from the pXRF are in percentages except for magnetic susceptibility* ($\times 10^{-8}$ m^3 kg^{-1}) *and pH.* ‡*according to Bruker Elementar S1 Titan fact sheet.* **Outside elemental range*

standard methods with equal amounts of air dried 2 mm sieved sample and distilled water. As for magnetic susceptibility, the high resolution resulting from the 0.25 m grid (Fig. 4a) was not assumed to be necessary for pH analysis and hence, the lower resolution 1.0 m grid was chosen here.

Statistical mapping

Following the laboratory analyses, a spatial analysis of the multi-element, MS and pH measurements was performed. The spatial analysis was performed using ordinary kriging using the software program "R" version 3.4.3 with add-on packages "sp", "gstat" and "raster". See Trant et al. (2021) for further information on the kriging and spatial analysis.

Soil and sediment micromorphological analysis

The thin sections were scanned using a flatbed scanner following Arpin et al. (2002). Observations were made using a petrological microscope under plane-polarized light (PPL), crossed polarizers (XPL), oblique incident light (OIL), and fluorescent light (FL) at magnifications of × 25, × 40, × 100, × 200, × 400 and × 500. The thin section descriptions follow the international nomenclature of the "Guidelines for Analysis and Description of Soil and Regolith Thin Sections" (Stoops 2003).

Artefact distributions

The excavation of the sediments has led to > 4000 artefact finds. Most were retrieved during systematic wet sieving (2 mm mesh) of all excavated sediment. The sieved finds were related to stratigraphic units ('A-units'), and within these to smaller find registration areas ('X-units'). As an additional procedure adopted for the intensively sampled floors that are the subject of this contribution, sediment samples from the units sampled for geochemistry were collected in 50 cm grid squares to be floated and wet sieved at 1 mm.

A relatively small proportion of the finds was recovered individually during manual excavation. These were measured with 3D coordinates if they were of outstanding character, if their potential for dating made it crucial to have full control over their stratigraphic position, or if their position

(i.e. likely in situ) might be informative of functional use of space. Coinage (i.e. sceattas) and loomweight fragments were the two main find categories that were systematically measured when observed in situ. The presence of bulky waste such as broken loomweight fragments indoors might indicate the position of the loom during the latest phase of occupation of a building before its abandonment.

The spatial distribution of loomweights, both fragmented and complete, was assessed using single measurements of in situ finds held against the pattern of loom weight distribution retrieved by sieving of sediments from the find registration areas of all the stratigraphic units represented in both buildings, K23 and K22c. In contrast, the distribution of selected find groups (vitrified fuel ash, animal bone, burnt clay, casting mould fragments and sherds of pottery of domestic type) was analysed by treating these groups in bulk (count/weight) and establishing quantitative variation across the sampled area on the same grid.

Results

Analyses of the bulk samples

Magnetic Susceptibility

Figure 5a shows the MS measured for the entire surface including both house phases (K22c and K23). It clearly demonstrates that the highest levels of MS are found within the area of house phase K23 included in the sampling (A264). House phase K22c also holds areas with increased MS, especially along the central aisle and in the back of the northwestern side aisle. However, metalworking will produce a stronger MS signal than heating, which might result in a masking of the heating signal if both activities have taken place and are included in the same dataset. Since metalworking has been recognized on-site and large concentrations of metal finds are measured in house K23, a new map of MS leaving out all samples within the area of A264 were performed.

Figure 5b shows the MS signal derived only from contexts covering K22c, plot margin (A266) and pathway/street (A243). Here, several areas with high MS are clearly shown. The front part of the central aisle exhibits several smaller increases in MS, and the back part of the central aisle displays a larger area with high MS. Additionally, high MS is found in the back of the northwestern side aisle and as a small area in the back of the southeastern side aisle. Neither the plot margin (A266) nor the pathway/street (A243) shows elevated levels of MS.

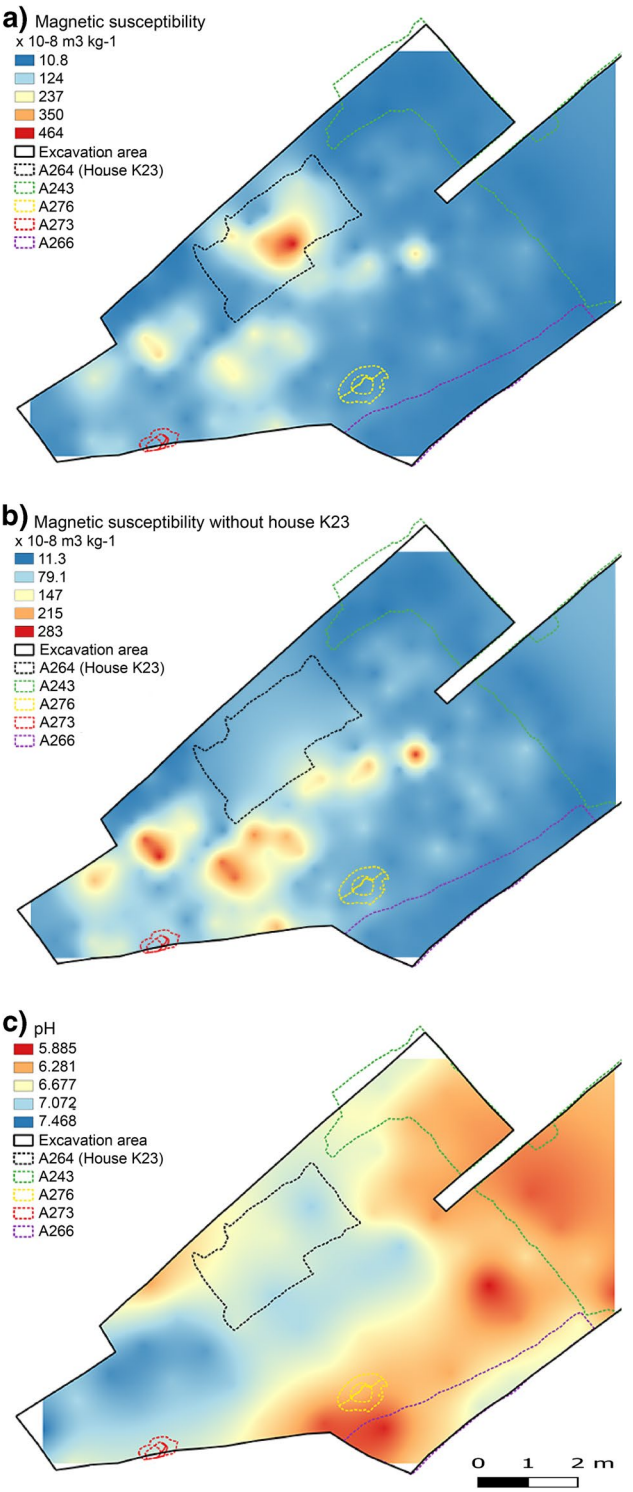

Fig. 5 **a**) Soil magnetic susceptibility of the entire surface including both house phases (K22c and K23). **b**) Soil magnetic susceptibility with samples from excavation unit A264 excluded

Soil pH

The soil pH varies from neutral to slightly acidic across the indoor area (Fig. 5c). The central aisle and the northwestern side aisle (including house phase K23) exhibit neutral pH values around or just above 7. Both front rooms have weakly acidic to neutral pH (pH = 6–7), with the southeastern front

room showing the most acidic values (pH = 5.9). The south-eastern side aisle also shows weakly acidic pH values, where one area with the lowest pH levels in the back part stretches into the plot margin area. The northern part of this area (A266) is neutral to slightly acidic and becomes somewhat more acidic towards the southern end. The pathway/street (A243) also displays slightly acidic pH values.

Geochemical analysis

All elemental mapping but sodium is based on pXRF, while results for sodium is based on ICP-MS. The results for all elements are treated as one in the following. For comparison of the different geochemical methods see Trant et al. (2020). Elemental concentrations are presented as percentages.

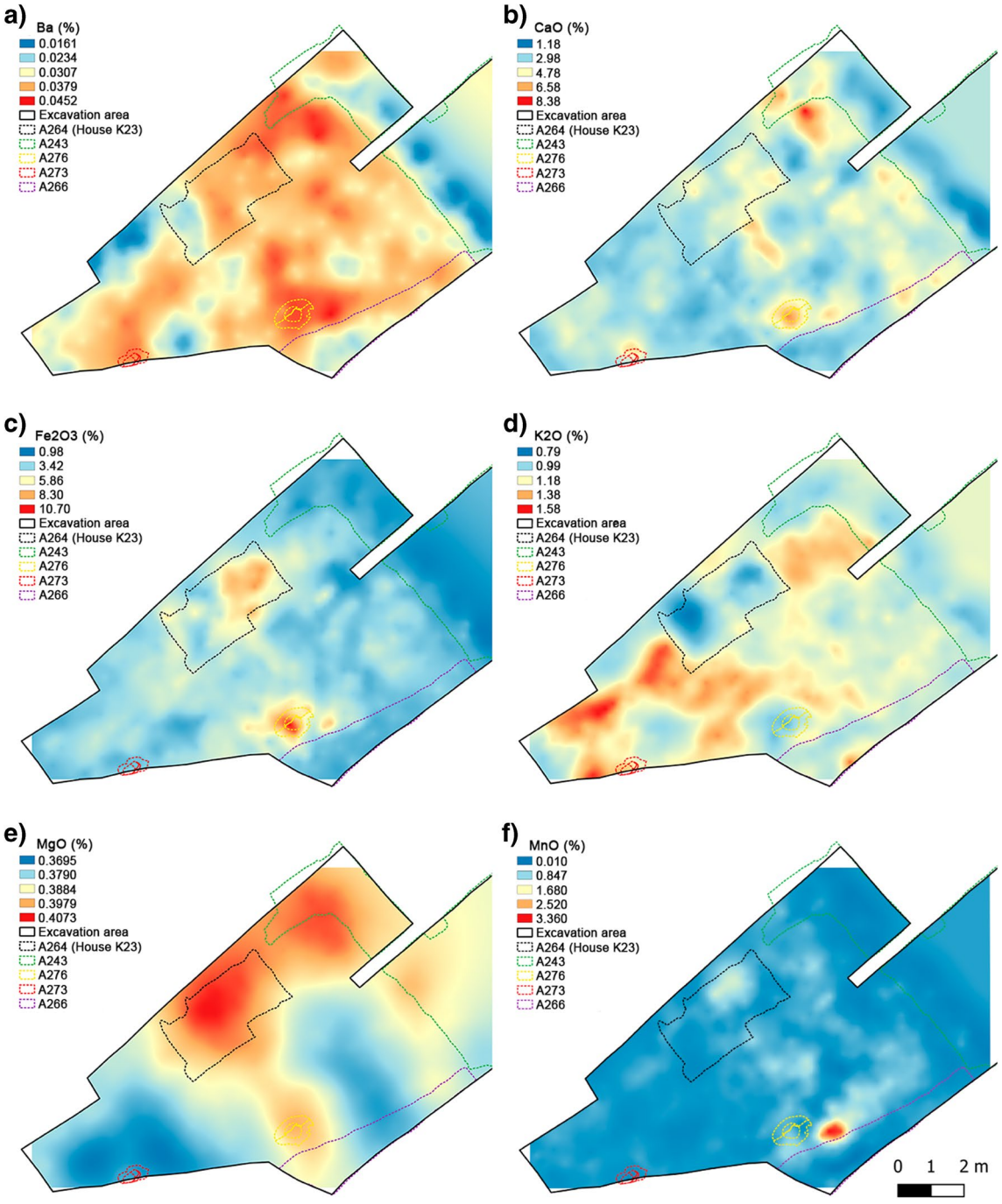

Fig. 6 Multi-element analysis of anthropogenic markers of the entire surface including both house phases (K22c and K23). a) Ba. b) CaO. c) Fe_2O_3. d) K_2O. e) MgO. f) MnO

Common anthropogenic markers *Ba*

Barium (Fig. 6a) generally shows high values across the entire house floor. Only two areas in the back part of the house display very low levels of Ba in the indoor area. The plot margin (A266) also holds high concentrations of Ba except for the southern most part, which has lower levels. The pathway (A243) features very low Ba-concentrations, especially in the eastern part.

CaO

Calcium (Fig. 6b) is most pronounced on the outskirts of the northern northwestern front room, where the highest concentrations of Ca are measured. This area is also the most widespread high-concentration area with Ca. Just southwest of this Ca-hotspot is a coldspot with low Ca-concentrations. Increased levels of Ca are also found in the southern southeastern front room, as a clear line across the central aisle and associated to the hearth (A273) and baking oven (A276). Lower levels of Ca inside the house are mainly found along the central aisle. House phase K23 generally does not hold increases nor decreases in amounts of Ca.

The plot margin area (A266) features a slight increase in Ca in the northern part, but also holds low Ca-values in the most southern part. The pathway/street (A243) generally shows very low levels of Ca, despite the northern corner around the house.

Fe_2O_3

Iron (Fig. 6c) occurs as two high-concentration areas inside the house. One area, with the highest concentrations measured, is at the same place as the baking oven (A276). The other high-concentration area is within the northernmost half of house K23 (A264). Lower concentrations of Fe inside the house area are mainly focused along the central aisle and down to the hearth area (A273) in the back end of the house. Hence, the main part of the indoor area does not include major variations in the Fe-levels.

The plot margin area encompassed low Fe levels, but without any fluctuations. The northeastern side of the pathway/street, featuring the outermost samples analysed, shows some of the lowest Fe-levels measured, but as for the plot margin area, without any major variations in the concentrations.

K_2O

The highest concentrations of K are found at the back of the house (Fig. 6d), as two larger areas stretching from the most southwestern end of the house and onto the centre of the central aisle and into the eastern part of the southeastern side aisle just above the baking oven (A276). However, this high-concentration area is interrupted by a low-concentration area just north of the hearth (A273). The northern part of the northwestern front room also holds an area with high K-levels. The area surrounding the baking oven (A276) features lower concentrations of K. House phase K23 as represented by A264 shows the lowest concentrations of K.

The plot margin area (A266) generally does not feature much variation around the mean concentration, beside one small area just on the excavation border with high levels of K. The pathway (A243) features slightly low values, and generally encompasses a slightly lower concentrations than the indoor area.

MgO

Magnesium (Fig. 6e) was only detected in 230 samples. It has a very high detection limit (> 0.49%) with the pXRF. Samples, with detected Mg are spread across the entire excavation area and include both house phases, plot margin and road street areas. However, areas reflected as low concentrations generally reflect undetected samples. High concentrations in the indoor area are reflected mainly in house K23 (A264), in the northwestern front room of house phase K22c and to some extent around the baking oven (A276).

MnO

High concentrations of Mn are only seen just above the baking oven (A276, Fig. 6f). The rest of house phase K22c generally displays very low levels with smaller increases, however, none of these exceeds the mean value. House phase K23 (A264) contains one area with a slight increase, but generally holds the same tendencies in Mn-concentrations as K22c. Both the plot margin and the pathway areas show very low concentrations.

P_2O_5

Phosphorus has its largest and most widespread high-concentration area around the baking oven (A276, Fig. 7a). Other P-hotspots are found in the northern part of the nothwestern front room and as two areas with elevated concentrations in the southeastern front room. Slightly enhanced levels of P are also found across the centre of the central aisle and to the very back of the house. Low levels of P are mainly found in the southwestern part of the central aisle. House phase K23 (A264) holds a smaller area with high levels.

The plot margin (A266) seems to contain two separated areas of P-levels: The northernmost part encompasses slightly increased concentrations, while the southernmost part's concentrations are somewhat lower than the mean concentration. The northern side of the pathway, holding the outermost row of samples, shows very low P-concentrations. However, these concentrations seem to increase going across the pathway towards the indoor area. Increased levels of P are found in the northern corner of the pathway area.

Sr

Strontium (Fig. 7b) shows several areas with enhanced levels above the mean inside the house. The most pronounced high-concentration area is around the baking oven (A276), which holds the highest Sr-levels measured. Both front rooms also show high concentrations, with the northwestern front room having slightly higher

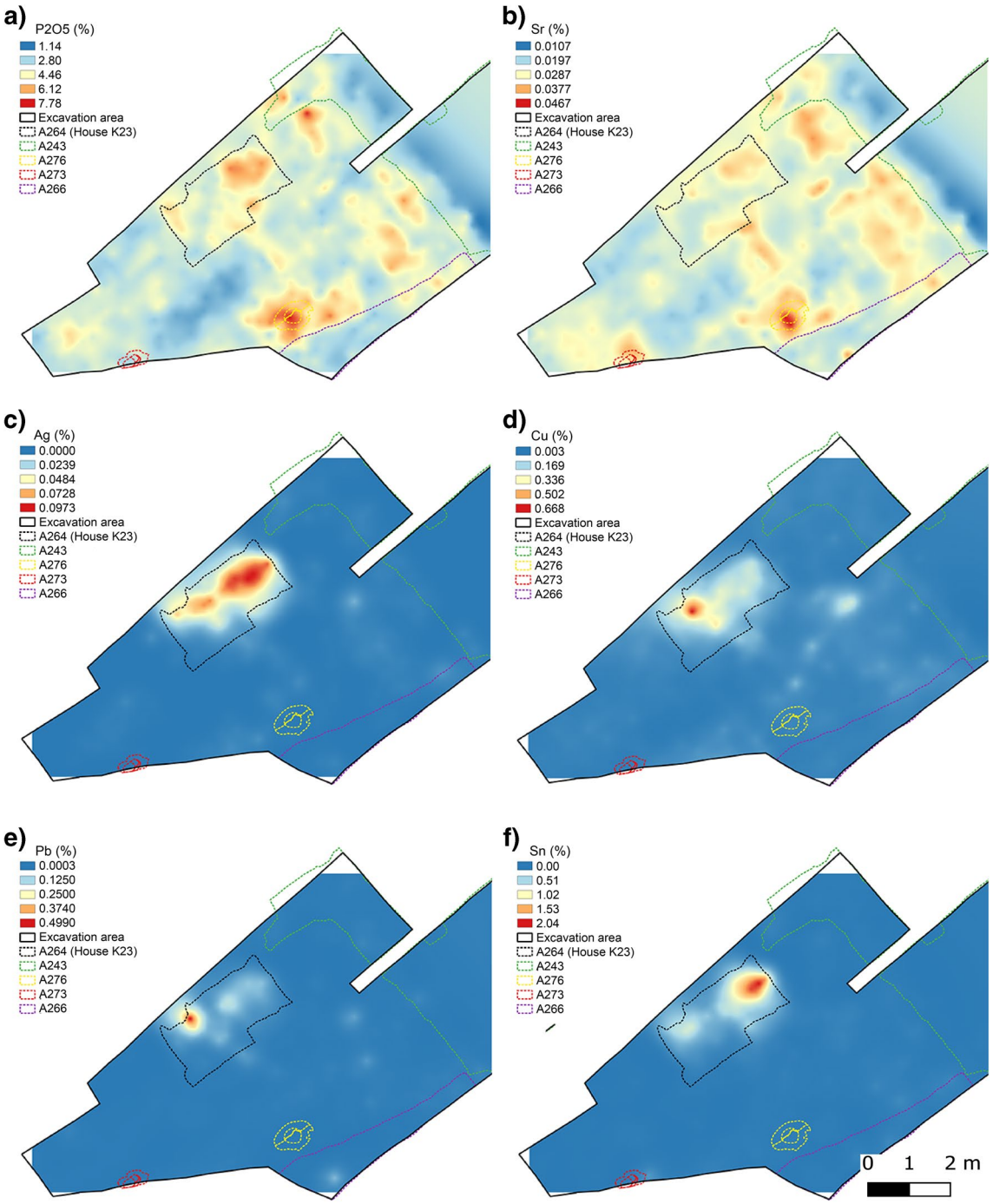

Fig. 7 Multi-element analysis of anthropogenic markers of the entire surface including both house phases (K22c and K23). **a**) P_2O_5. **b**) Sr. **c**) Ag. **d**) Cu. **e**) Pb. **f**) Sn

concentrations than the southeastern. Enhanced concentrations are also found in the centre of the central aisle and at the hearth (A273). Low Sr-levels are found especially in the southern part of the central aisle, but also in the southern part of the northwestern side aisle (below A264) and in the eastern part of the southeastern side aisle in between the high concentrations from the baking oven and front room areas. House phase K23 (A264) shows a smaller area in the northern part with increased Sr-concentrations. In the southern part of K23, concentrations are below the mean.

The plot margin area generally has Sr-concentrations around the mean value, beside two very small areas (approximately 0.5 m in diameter) with high concentrations. The northern side of the pathway/street shows very low Sr-levels, with the lowest ones being in the eastern end around the sand patch (A265).

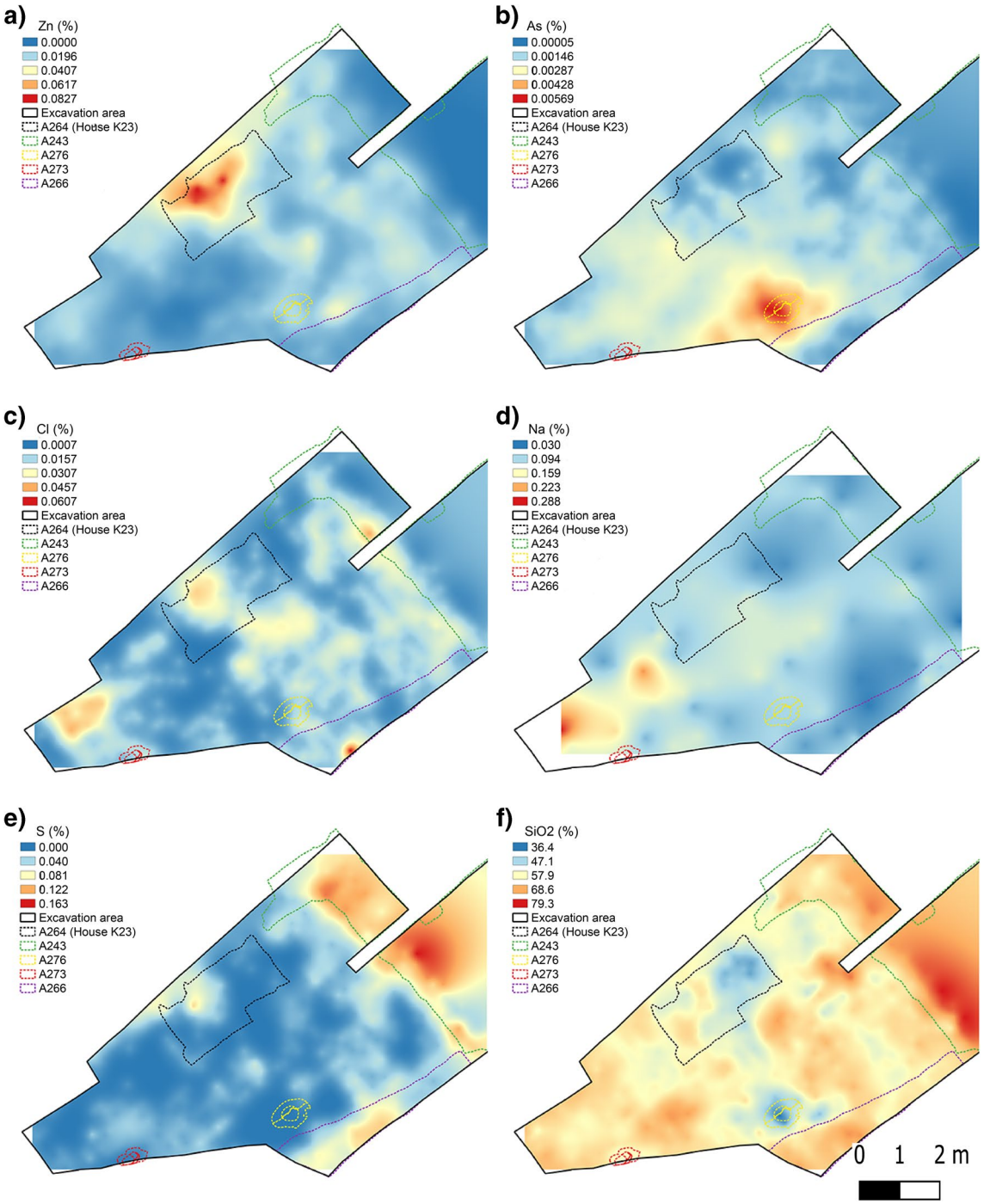

Fig. 8 Multi-element analyses of anthropogenic markers of the entire surface including both house phases (K22c and K23). **a**) Zn. **b**) As. **c**) Cl. **d**) Na. **e**) S. **f**) SiO_2

Metals Ag (Fig. 7c), Cu (Fig. 7d), Pb (Fig. 7e), Sn (Fig. 7f) and Zn (Fig. 8a) all show a hotspot-tendency as only occurring with very high concentrations in house K23 (A264).

High Ag-concentrations stretch across K23, going from north to south, but with the highest levels in the northern part of K23. Cu is mainly concentrated as a very small hotspot-area in the southern end of K23. As for Ag, elevated Cu-levels stretch towards the northern end of K23, but not as pronounced for Cu. The high concentration of Pb is located at the same place as Cu in the southern side of K23. The Pb-hotspot is also very small in extent, showing a diameter of only 0.5 m. Slight increases in Pb-concentrations can be

found moving from the hotspot and towards the northern part of K23. However, these concentrations do not exceed the mean value of Pb. High levels of Sn are mainly concentrated in the northernmost part of K23, with a small increase in the concentrations in the southern end of K23.

Zinc shows highest concentrations across the area of K23, filling out approximately half of the surface area of this house phase. Contrary to the other metals concentrated in K23, Zn also shows smaller rises in concentration across the area of house phase K22c. These enhanced areas are mainly found in the front rooms and in the eastern SE side aisle; however, none of them exceeds the mean value of Zn.

Other elements *As*

Arsenic (Fig. 8b) has one large area with high concentrations surrounding the baking oven area (A276). In the rest of the house, concentrations are generally low. The back part shows concentrations around the mean and the front part displays smaller fluctuations with concentrations below the mean. House phase K23 (A264) shows very low levels of As.

Both the plot margin (A266) and the pathway (A243) feature low As-concentrations.

Cl

Chlorine (Fig. 8c) shows several areas with smaller increases in the concentrations, especially in the two front rooms, the central aisle and northeast of the baking oven. Highest Cl-concentrations are found in the back part of the house, where concentrations exceed the mean in a relatively large area. House phase K23 (A264) also encompasses an area with increased Cl-concentrations. Since Cl concentrations are the lowest nearest the present-day street Sct. Nicolaj Gade, contamination with modern road salt (NaCl) seems unlikely.

The plot margin area (A266) features one small area with very high concentrations, however, this Cl-hotspot only originates from one sample. The pathway (A243) generally appears to be low in Cl, but with increased concentrations in the border zone between the indoor and outdoor areas.

Na

Sodium is measured with ICP-MS only, as opposed to the other elements that are pXRF-based. Consequently, Na is only measured in 104 samples, which do not cover the full extent of the house, and hence, the kriged map (Fig. 8d) does not show predictions for the entire excavation area. Concentrations of Na are generally low across the indoor surface, but smaller increases can be seen along the central aisle. In the back part of the house, one large high-concentration area can be found together with a smaller one to the northeast.

Both outdoor-areas, plot margin (A266) and pathway/street (A243), show low Na-levels.

S

Sulphur was only detectable in half of the samples. Most samples holding detectable concentrations are found in the plot margin and pathway areas, which is also reflected by Fig. 8e showing very low concentrations across the entire indoor surface. Only a small area in house phase K23 (A264) displays higher S-concentrations.

The plot margin (A266) features high levels of S in the middle part and stretching towards south. In the pathway (A243), the highest S-concentrations are measured. Generally, the pathway holds very high levels of S.

SiO_2

Most of the indoor area encompasses Si-levels above the mean (Fig. 8f). The central aisle shows levels slightly higher than the rest of the house area. The lowest levels of Si are found around the baking oven. Low Si-levels are also found in the northwestern front room, in the middle of the central aisle and as smaller spots in the side aisle. House phase K23 (A264) holds one larger area with Si-concentrations as low as the ones around the baking oven.

In the plot margin area (A266), Si-levels are high in the southern end. The pathway/street (A243) shows very high levels of SiO_2 in the eastern end, which is also where patches of light sand (AA65) was found on site. In the northern end of the pathway, Si concentrations are only slightly higher than the mean.

Based on the geochemical distribution maps, Plot 1 is divided into several areas describing different possible activity areas (Fig. 9).

Micromorphology

In the following, the main micromorphological results are presented. For additional information and description of microstratigraphy, see Croix et al. (2022) and Wouters (2022). For this particular case, descriptions and interpretations were organised per stratigraphic unit *in lieu* of applying the concept of microfacies (Courty 2001), since the horizontal variations in composition and character would render the list of sub-microfacies too elaborate; and would potentially obscure meaningful horizontal differences. However, a characterization of the most important fabrics can still be made in order to introduce the most commonly encountered components on site.

Five main fabrics could be distinguished on site. Fabric 1 (e.g. units A262 or A263 as can be seen in Fig. 10) is the most common, and characterised as a predominantly fine to medium sand with a $c/f_{10\mu m}$-ratio of 80:20 to 70:30. The micromass of this fabric is usually composed of fine organic matter, microcharcoal and minute anthropogenic inclusions, as well as inorganic residues

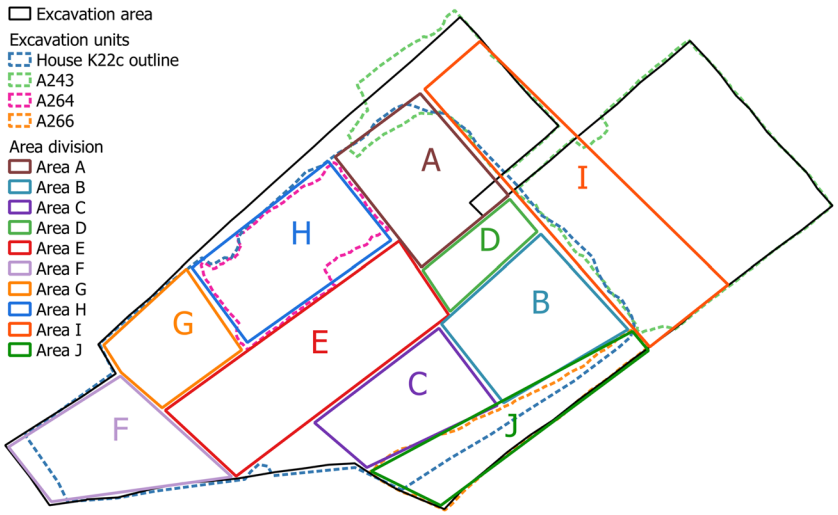

Fig. 9 The sampled area is divided into 10 areas based on the geochemical distribution of elements, suggesting different uses of space inside and outside of houses K22c and K23

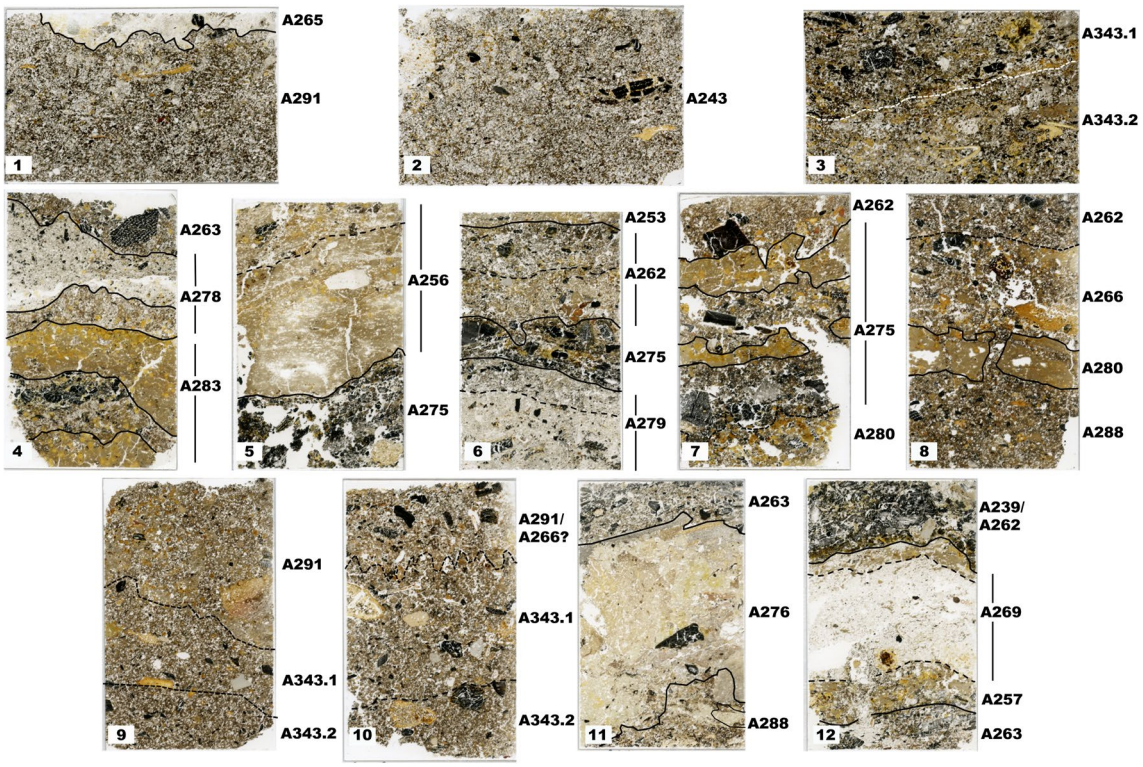

Fig. 10 Thin section scans of thin sections 1–12 with recognized excavation units

of organic origin (predominantly phytoliths). The coarse fraction also includes varying concentrations of chert, and of anthropogenic inclusions, such as charcoal or charred grains, bone and fish bone in various states of burning or weathering, non-metallurgical slag, pottery fragments, silty clay aggregates, and sometimes metal slag. Locally, better preserved organic fragments can still be identified as bark chips or shavings and grass stems. Phosphatic and iron features are common in this fabric. Fabric 2 (e.g. units A280, A281 or A283) is composed predominantly of silty clay with abundant diatoms, at times tempered with unidentifiable strands of organic matter. Some phytoliths and faint traces of fine anthropogenic inclusions, such as charcoal, can sometimes also be discerned. Pedofeatures are usually limited to phosphatic infillings and orthic iron nodules. Less common is Fabric 3 (e.g. unit A276), which is composed predominantly of silt to fine sand, and is highly muscovite-rich (and glauconite rich), in contrast to the

diatom-rich clay as found in Fabric 2. Fabric 4 (e.g. unit A265) is a predominantly fine to medium sand composed mainly of the silicious fraction of decalcified ash, locally mixed with some sand or silty clay. This fabric contains abundant phytoliths, sometimes in a blackened or molten state, and microcharcoal. Fabric 5 (e.g. unit A275 as can be seen in Fig. 11) is composed nearly solely of charcoal interspersed with fine to coarse sand, and locally anthropogenic inclusions.

Artefact distributions

A total of 4105 artefact finds and 9.0 kg of animal bone were recorded from the floor area of K22c and the sampled parts of K23, in addition to 3148 finds and 70.4 kg of animal bone from the adjacent pathway/street area and plot margins (Fig. 12). A large part of the find assemblage in K22c/K23 comprises refuse from non-ferrous metalworking, including 658 casting moulds and 147 crucible fragments, 488 pieces of vitrified clay and 325 pieces of metal slag. Other crafts are represented by relatively insignificant amounts of finds, for example only 12 fragment pieces of debris from bone- and antler working and 26 pieces of glass-working debris. This absence is notable, as levels from the building immediately prior to K22 on the plot, K21, were associated with thousands of finds related to the latter two crafts. This is a clear testimony to the integrity of the stratigraphy, and to the fact that the majority of artefact finds from units associated with building phases K22c/K23 are related to activities contemporary with this horizon, with a relatively minor proportion of intrusive or residual objects. For additional information see Deckers (2022). Other major find groups include 1299 fragments of burned clay, mainly material from ovens, 360 pottery sherds and 242 pieces of

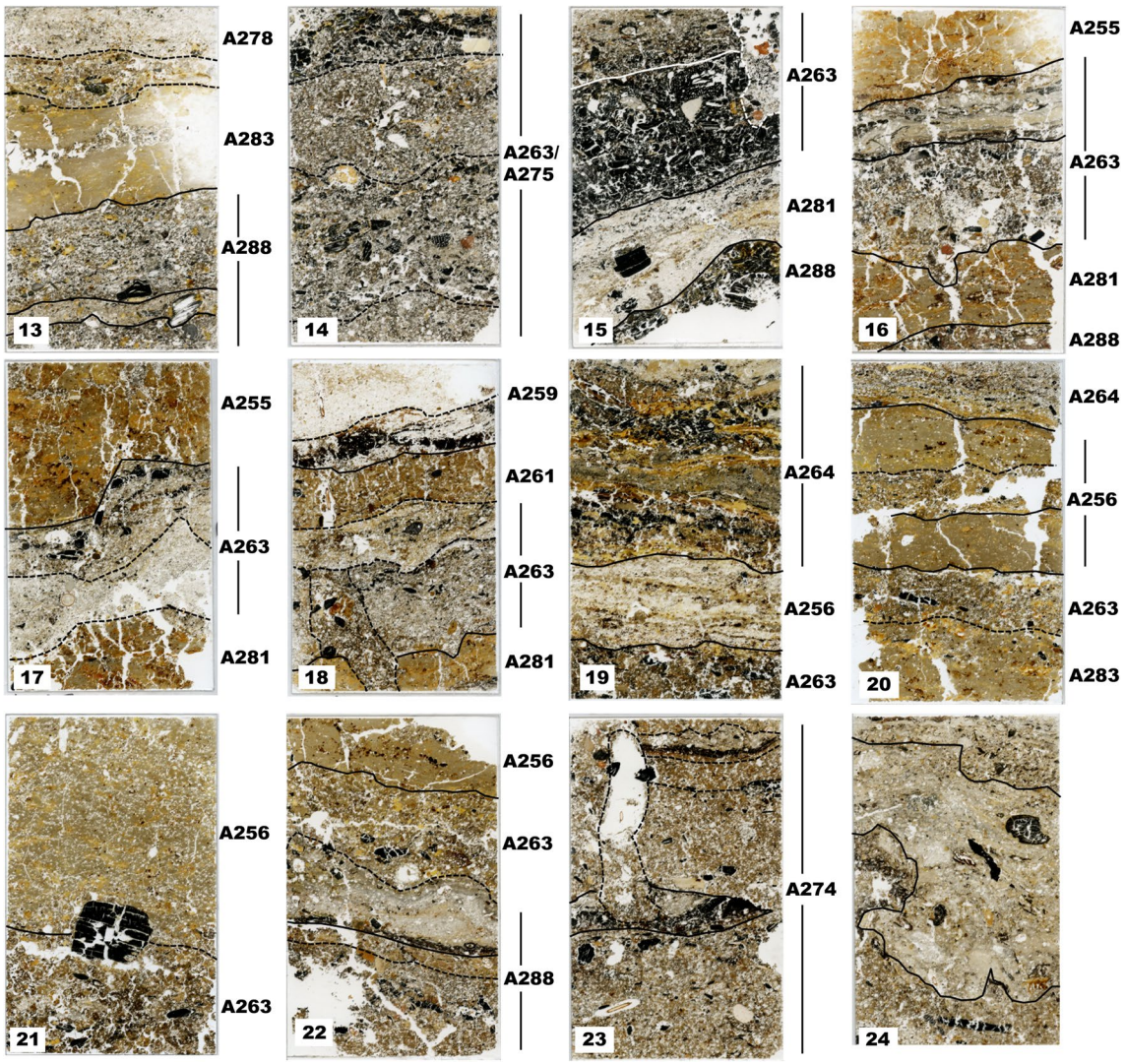

Fig. 11 Thin section scans of thin sections 13–24 with recognized excavation units

Fig. 12 Artefact distributions of the sampled surface including both house phases (K22c and K23). **a**) Loom weights associated to K22c. **b**) Loom weights associated to K23. **c**) Vitrified fuel ash (counts). **d**) Animal bone (weight). **e**) Burnt clay (counts). **f**) Casting moulds (counts). **g**) Casting moulds (weight). **h**) Pottery of domestic type (counts). C-H shows artifacts recovered from 0.5 m × 0.5 m grid sampling of large bulk samples retrieved from the same layers as the geochemistry bulk sampling

iron (mostly corroded beyond recognition). Domestic activities are probably indicated by personal objects and dress ornaments including 51 fragments of glass vessels, 30 glass beads, 38 loom weight fragments, and objects such as spindle whorls, a decorated bone or antler comb, a copper-alloy brooch and a coin (Fig. 13).

The distributions of selected groups of artefacts show spatial trends (Fig. 12). Metalworking debris is found throughout, though most prominently in areas A-D and H (see below). As discussed above, areas A-D showed poor separation between materials from building K22c and K23, and finds from this area may relate to the occupation of K23 contemporary with Area H. Some of this material could have been levelled from refuse heaps in connection with building refurbishments and floor maintenance. Meanwhile, a group of domestic objects show a clearly different trend. In K22c, loom weight fragments concentrate strongly in and around Area F, suggesting that a loom was placed here along the west wall. Beads and individual personal objects including a comb and a brooch cluster in the same area.

Discussion

This section addresses both main aims of this study – namely a better understanding of the complex stratigraphy of Plot 1 containing K22c and a part of K23; as well as an interpretation of house extent and activity areas. In the latter, the results of all analyses are grouped spatially per house area or specific feature.

Taphonomic Processes

Soil water fluctuations

The strata presented here have been subjected to significant fluctuations in water content over time. This is in contrast to the older site phases from approximately 700 to the late 750s where organic material was relatively well preserved due to continuous, near waterlogged anoxic conditions resembling those described by Breuning-Madsen et al. (2001), where localized, wet, anaerobic conditions arose in the core of an experimental buried mound due to oxygen depletion as a result of decomposition of plant remains. The fluctuations in water content are evident from a poorly preserved, and in some areas completely decomposed (absent due to oxidisation), organic component, despite the fact that the older phases (before c. AD 750) suggest a very high input of organic matter in among other flooring and building materials on the site, including wood, wattle, straw/reed, heather, moss, and others. Apart from the poor preservation of organic materials, pseudogley in heterogeneous, organic-rich patches (Kristiansen & Tjelldén, 2022) is attested by phosphatic pedofeatures, such as infillings, coatings, and nodules (Karkanas & Goldberg 2018), with particularly vivianite and pyrite most abundantly present in former outdoor or liminal areas, such as the pathway/street or house entrance. Past reducing conditions are also indicated by microscopically visible redoximorphic features, such as iron nodules, hypocoatings, and the banded iron staining of clay, where reddening was not attributed to heating (Vepraskas

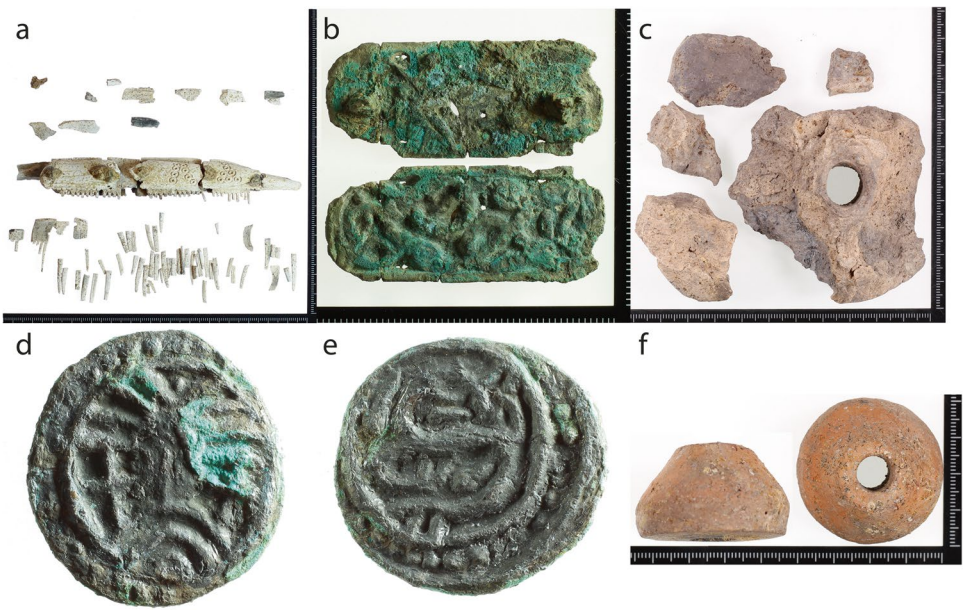

Fig. 13 Artefacts from the floors and activity layers of K22c and K23. **a**) A fragmented, burnt antler comb of Nordic type (find ID A263X646). **b**) A copper-alloy rectangular brooch with geometric animal design (A264X2162). **c**) Fragments of one or more loomweights in fired clay, with a characteristic donut shape. **d** and **e**) A silver coin (sceatta) of the Wodan/Monster type, probably minted in or near Ribe (A256X573). **f**) A ceramic spindle whorl (A263X647)

et al. 2018). The results of modern oxidation are most pronounced in the southwestern area of the site, likely due to a combination of relatively thin deposits and post-depositional disturbance due to an old excavation trench and a small, uncobbled, urban garden. For preliminary assessment of the site' in situ preservation conditions based on macroscopic evidence, see Kristiansen & Tjelldén (2022).

Ash taphonomy

A progressive decalcification of plant and wood ash was observed. Only in very rare occurrences did the ash retain its anisotropic properties or calcium oxalate crystals. Elsewhere, near-isotropic areas were locally present, likely resulting from phosphates from dissolving bone or degrading organic matter, converting ash calcite into apatite or other phosphates (Canti & Brochier 2017). An alternative explanation is that these are ashes of non-woody plant or of herbivore dung consisting mostly of phytoliths, molten phytoliths and charred remains, with little or no carbonates. Most often, however, the ash at the emporium site had become completely decalcified, leaving behind only a mineral component consisting of silica bodies, non-metallurgical slag (vitrified ash), (micro)charcoal or mixed in fine sediment. This is due to the localized acidification of the soil, continuous leaching and very heterogenous redox conditions producing additional protons.

Bioturbation

The levels of faunal bioturbation were variable – relatively limited in units rich in silty clay, charcoal or decalcified ash, but more thorough in deposits previously rich in organic matter. It is represented by mesofaunal channels, local chambers, and excremental organo-mineral micro-aggregates (Kooistra & Pulleman 2018), especially in the units where organic remains were still present. In older house phases at the site, lower down in the stratigraphy, beetle and mite excrements were present (Wouters 2022), but these could not be observed in the house phases analysed here, possibly due to poor preservation conditions for organic matter. Bioturbation by ants is attested in a younger phase on site dating to the second half of the ninth century (Wouters 2022), but could not be ascertained in this phase.

Traces of past plant rooting were rather limited as well, and mostly encountered in outdoor areas. Modern rooting evident from its better preservation and birefringence under XPL (Ismail-Meyer et al. 2018) was more abundant. It was most strongly concentrated towards the south and southeast of the excavation trench, where a modern patch of greenery was located before and at the time of excavation. This affected areas J, C, F, and the southwestern part of E most profoundly.

Physical alterations: compaction, sinking, structural deformations, floor maintenance practices and truncations

Several types of physical alterations could be discerned. First, due to the use of space in the built area of the plot in older phases, several areas were prone to deformation or structural collapse. Deformation was especially visible in the side aisles of buildings, leaning down towards the plot margins surrounding them on both longitudinal sides. Most likely due to the compaction and decomposition of organic matter originally in side aisles and plot margins, this deformation caused challenges for the archaeological attribution of stratigraphic relationships, especially when connecting indoor and outdoor strata, as well as for the geochemical sampling (see Trant et al. 2021). The presence of sunken-featured buildings in older phases also caused a structural prone-ness to collapse.

Next, anthropogenic activities related to the maintenance and (re)building of buildings played a significant part. In several locations, units have been truncated due to the removal of material. This could be related to the removal of house floors that had built up during use, since (vitrified) plant and charcoal ash, as well as combustion waste, were regularly spread on the floors (Milek & French 2007; Milek 2012). Layers of decalcified ash were thickest, or best preserved, along the outer walls, where they may have been swept to, or where they may have been less prone to wear (Banerjea et al. 2015; Macphail et al. 2004). Amongst the finds from the sieved bulk samples, vitrified fuel ash displayed a relatively even distribution all over the sampled area. These fine, unobtrusive particles would have been difficult to sweep or otherwise remove as part of floor maintenance and are thus found across the floors of both K22c and K23. The patchy nature of this distribution, with apparent concentrations near hearths and in the northern entrance area, may reflect the nature of flooring (presence or absence of clay floors) as well as the management of ash.

Organic components such as grasses, or wood or bark chips were likely used as floor cover in certain areas as well. This practice of removing growing house floors is ethnographically attested from the North Atlantic region (Milek 2012). Other truncations are more likely the result of removing older material prior or during the erection of new buildings, as was the case for parts of unit A263 (K22c), after which the clay floors of K23 were laid down. This is most visible in Area G. Older evidence of house fires may have been removed by such truncations, as hypothesised for (part of) older house phase K22b. In addition, problems of separation between house phases were most commonly encountered in areas without clay floors (see "Spatial analysis of the house and its surroundings" section), such as entrance area D and areas B, C, I, and J.

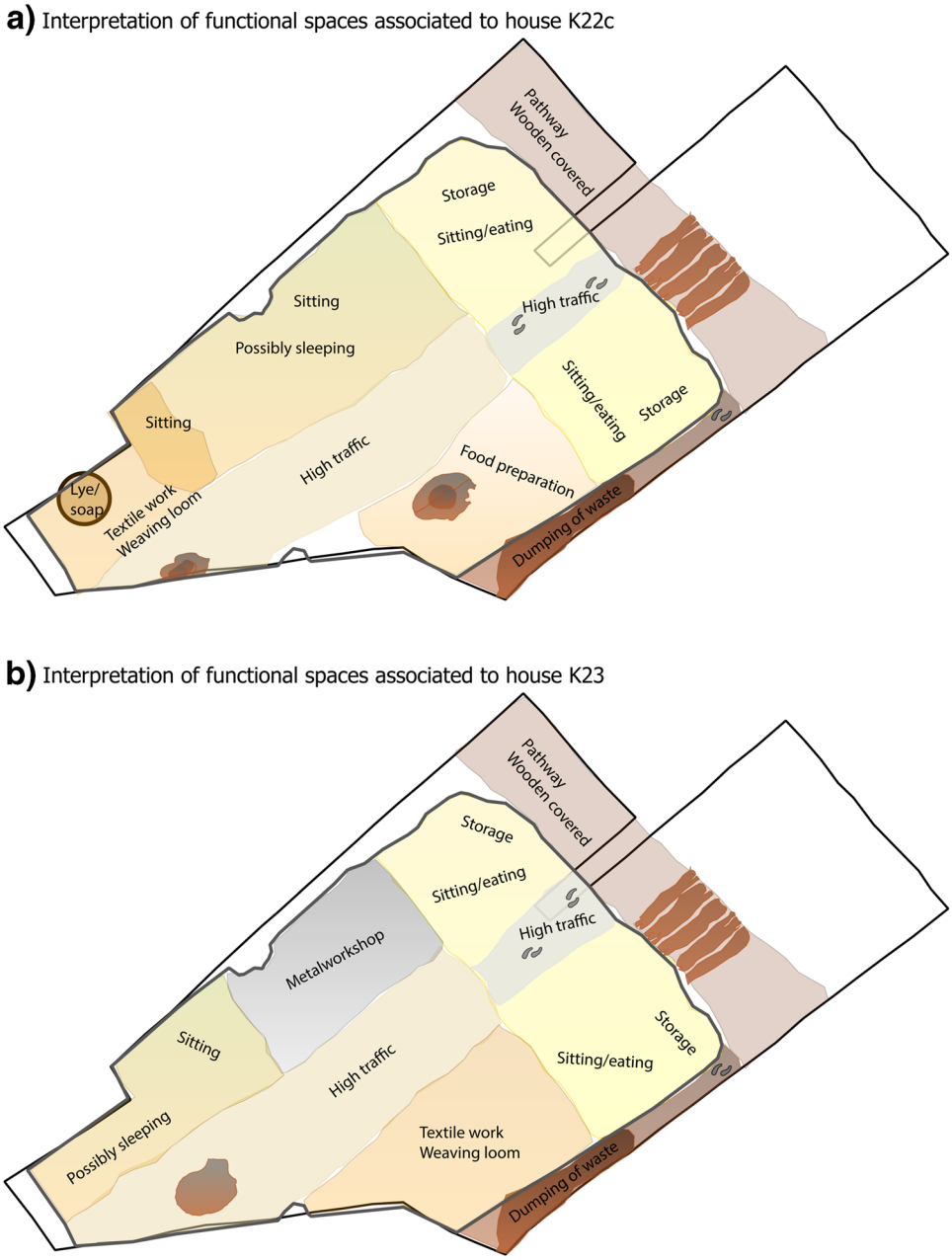

Fig. 14 Interpretation of the use of space associated to the two houses K22c and K23. **a**) House K22c had a more domestic appearance, including an area with designated space for food preparation with a baking oven as well as space for textile working with a weaving loom and possibly storage of lye or soap. **b**) House K23 also encompassed textile working with the possible presence of a weaving loom, in addition to a space for a metal workshop. Both houses had an entrance area and central aisle with traces of high traffic as well as two front rooms that might have been place for storage and/or sitting and eating. In front of the house was a wooden trackway and south of it the plot margin, resembling a shallow ditch where waste associated to the house activities was discarded

Spatial analysis of the house and its surroundings

Area A—NW front room

This area is interpreted as the potential location of storage (Fig. 14a)**.** The area corresponds to the western front room of the houses, with micromorphological data available from both house phases. The geochemical data refer to the occupation deposit of older house K22c, locally mixed with remains from K23 where they could not be distinguished (A279, A262). For these units, the chemical elements of the part of the house near to the outer wall (high Ca, Ba, Mg, P, Sr, K, Zn decreased Si) may be representative of household waste, and different types of combustion waste or ash. The micromorphology and field observations show thicker depositions of ash near the outer walls, either due to sweeping, or due to more significant wear away from the walls (Banerjea et al. 2015; Macphail et al. 2004). They also represent nutrients, which is consistent with the evidence of organic floor cover in thin section. Due to the strongly decayed state of the floor cover, only a few bark fragments could be identified, but otherwise no identification of plant parts or species was possible. Micromorphology shows a gradual accumulation of both combustion waste in the form of charcoal, decalcified ash, and non-metallurgical slag, as well as fragments of unidentifiable organic matter. They

overlie a dump of well-sorted ash and sand, which in turn lies on a sequence of a silty clay preparation layer and walking surface, truncated by another silty clay layer (A283a-c).

Multiple occupation surfaces with slightly different proportions of sediment, charcoal, sand, decalcified ash and clay could be identified (minimum 3), that later became truncated by units belonging to house K23. A horizontal orientation of elongated components and the presence of rounded soil aggregates indicate that the surface was trampled, with a possible input of outdoors materials on shoes (Banerjea et al. 2015; Rentzel et al. 2017). The same sequence is visible in the central part of Area A, however, the geochemical signal here is "cleaner" (low concentration Ca, Ba, P, Si, Sr, increased concentration Fe, Mg, high K). This is likely due to the higher amounts of charcoal in the occupation surface at this location, which is probably linked to maintenance practices. No explicit indications for the area's use are apparent from the geoarchaeological data, although bone remains were observed in thin section. In the thin section closest to Area D, bark or other plant cell fragments, as well as burnt bone and fish bone were clearly present. The artefactual evidence (Fig. 14) demonstrates that animal bone fragments were present in two distinct concentrations in both front rooms (Area A and B), closely matching the P and Sr enrichment observed there (Fig. 7). The distributions might reflect physical boundaries within the internal space, which affected the movement of waste material, e.g. in the northeastern corner of the house or the northern entrance area. Animal bone also accumulated just outside the house walls, and tiny amounts (never exceeding 10 g per sample) can be found throughout the areas associated with K22c. Pottery sherds of domestic type similarly reflect the division between internal and external space, while a concentration in the eastern front room could indicate, together with the animal bone, the overall messy nature of this area.

Area B—SE front room

In the SE front room, the picture is somewhat similar to that in Area A (Fig. 14). The micromorphological data cover both house phases, starting with a thick layer (> 3 cm) of dumped, mixed combustion waste consisting largely of decalcified ash and some charcoal fragments in house K22c (A279) in thin section 6. This is followed by a series of indoor, trampled walking surfaces (Rentzel et al. 2017). The matrix of the lowest surface contains abundant charcoal fragments, with some clayey aggregates possibly brought in on shoes (Banerjea et al. 2015), as well as two small metal slag fragments. It is truncated by a maintenance layer containing a mix of clay and various concentrations of wood and plant ash (Matthews 2010) deposited in horizontal bands, followed by a walking surface rich in microcharcoal, organic matter ash, and bone remains. In thin section 7, plant tissue as well as animal bone and pottery are relatively well represented, more abundant and coarser than in Area A. This might be related to storage of foodstuffs, but potentially also to consumption. Over 90% of the pottery in K22c/K23 consists of simple, hand-made pottery. This is also the unit that was captured in the geochemical analysis (A275). Generally, this unit contains high concentrations of Ba, Ca, P and Sr together with increased levels of Zn and acidic pH, which might correspond to household waste or different types of combustion waste. The elemental distribution does to some degree resemble that of Area A, however, in Area B they do not appear with the same amounts of nutrients or elevated concentrations, indicating possibly a walking surface maintained with combustion waste. During the excavations both front rooms appeared 'messier', or maintained with less care.

Area C—Food preparation

This area is interpreted as a food preparation area in K22c (Fig. 14a). In its centre, remains of a baking oven were preserved. However, the lack of magnetic susceptibility elevation is striking. Thinsection 11 shows the presence of baking oven detritus in multiple phases and contains evidence of repeated destruction and re-use. Silica gel derived from molten phytoliths, as well as husks and blackened cereals are present throughout (Canti & Brochier 2017), embedded in a matrix of silty to fine, muscovite-rich sand. This matrix poses a stark contrast to the diatom-rich silty-clay that was used for flooring or reparation levels found elsewhere in the house. This is covered by a walking surface composed of a mix of decalcified plant and charcoal ash, and the remains of organic matter, probably related to younger house K23. Around the baking oven, the geochemistry contains large amounts of common anthropogenic and food markers (Ca, Fe, P and Sr). Some elements (As, Ca, Fe, Mg, P and Sr), all but As representable for foodstuff, show high concentrations exactly at the place of the baking oven (Figs. 6, 7 and 8), while K and Si appear to be very low in concentrations here. The distribution of burnt clay fragments shows a strong correlation with the oven A276. East of this, a small hotspot-area with high Mn-concentrations is found. The high-concentration elements as well as a low pH correlate well with plant remains and charcoal-rich ash, and the low Si could possibly be linked to the sediment mainly consisting of food-related ashes or deposits, which in combination with the micromorphological and archaeological evidence correlates with the area being used for food preparation. This is the only area in which As and Mn show high concentrations, possibly displaying a link between As and Mn concentrations and food preparation.

In the southwest of Area C, this same walking surface contains abundant charcoal, combustion waste, fresh organic matter and diagenised bone fragments. The materials and

sediment were accumulated gradually, and support an indoor area rich in organic matter floor cover or used materials (Banerjea et al. 2015; Lisá et al. 2020; Milek & French 2007); however, significant post-depositional bioturbation has heavily affected this part of the site. Contrary to other parts of Area C, the southwestern part is not rich in general foodstuff markers, with general low concentrations of Ca, K, Mg and Si. The low concentrations of Ca together with acidic pH around 6.3 correlate well with the diagenised bone fragments recognized in micromorphology. Low Si concentrations probably correlate with the deposit containing large amounts of charcoal and other non-silicate material. The area does contain high levels of As and Ba, which appear to be a general signal for this entire area. The geochemical distribution indicates that this part of Area C is on the border to where food was prepared.

The transition to house K23 is represented by a thick layer of sand bounded by thin clay layers at its bottom and top and contains two metal slag fragments at its bottom. A concentration of loom weight fragments was found in Area C associated to the upper level of building K23, which had already been excavated at the time of sampling. This might indicate the position of a weaving loom in this area, and it might have been contemporary to the metal workshop designated as Area H.

Area D – Entrance

This area is interpreted as a high-traffic entrance area, which appears narrower in house K22c than in house K23 (Figs. 3 and 14). This is based on thin section 13, which contains a clay floor, otherwise absent from thin sections in this area. In the very front part of the house, both K22c and K23 were captured in thin section, while the central part only contains units belonging to K22c. Whereas the central part is the result of repeated trampling, floor maintenance by spreading combustion waste and an organic floor cover, as well as potential regular sweeping or repeated truncation, the front part is a more transitional area with larger fragments of debris embedded in the sedimentary matrix, where wetter, 'dirtier' conditions persisted, especially in house K23 (Banerjea et al. 2015). The entrance area similarly has lighter artefacts fragments, stemming from increased trampling and fragmentation. Outside, the average weight of casting mould fragments in the pathway (Area I) and plot margins (Area J) similarly reflects greater and lesser trampling.

The northeastern part of Area D contains high concentrations of common anthropogenic markers such as Ba, Ca, P and Sr, which might indicate intensive use as suggested by Cook et al. (2014). Most of Area D holds relatively high concentrations of Si, possibly correlating with higher amounts of sand and phytoliths recognized in thin section.

More centrally in the area, represented by thin section 14, it was difficult to distinguish the different units belonging to K22c. A thick, gradual accumulation of several walking surfaces was not separated by clay floors or significant sand levelling layers, in contrast to thin section 15 or the rest of Area E further to the south. Four subunits could be distinguished, of which the lowermost and next to topmost contained a more significant organic matter component. This included phlobaphene-containing tissue, possibly related to bark chips or shavings being spread as floor covering. The other two subunits contained more charcoal and combustion waste, and generally coarser-sized anthropogenic inclusions, such as bone, charcoal, or clay aggregates. They show a combination of combustion waste dumping episodes and trampling. Locally, a high degree of in situ fragmentation of larger charcoal pieces indicates that larger quantities of ash were once present, but have leached out (Huisman et al. 2020).

Horizontal orientation of elongated fragments and features suggesting trampling were present in all subunits, attested by the in situ breaking of elongated components and planar voids (Rentzel et al. 2017). Locally, fragments were pressed into the matrix when softer, possibly sometimes damper, conditions prevailed. A diverse range of anthropogenic materials was observed – including small amounts of crucible fragments, clay and soil fragments, metal slag, pottery, and a minute coloured glass fragment. This may be related to higher amounts of loss, as well as inclusions brought in on the soles of feet, due to high traffic. Lithological discontinuities, attested by locally sharp boundaries, may indicate the removal of material as part of maintenance practices (Milek 2012). Bioturbation by mesofauna and root action is very limited in this area. In general, the southwestern part of Area D contains low concentrations of most chemical elements, and appears to be kept relatively clean, only containing high concentrations of Ba and Sr and high values of magnetic susceptibility. The low concentrations of Si might correlate to the limited amounts of clay or sand recognized in micromorphology. The clean geochemical signal in the area could reflect the intensive usage of a walking surface, not allowing much chemical remains to settle, but more likely, the geochemical signal is due to sampling height, which corresponds to the topmost subunit recognized in thin section as rich in mainly charcoal.

Area E – High-traffic central aisle

This area is interpreted as a high-traffic area in the central aisle of the house K22c (Fig. 14a). A marked difference exists between its northern half, with non-clayey thin section 15

on the one hand, and its southern half, with silty clay floor rich thin sections 16 and 17 on the other. Thin section 15, closest to the entrance area, is composed of a preparation or repair layer (A281) consisting of a lamination of sand, followed by fine sand mixed with clay and traces of ash, and a second sand layer, of which the top is mixed with charcoal and non-metallurgical slag remains. Next, a thick layer (A263) composed almost solely of charcoal is present, with a horizontal orientation of elongated components. Sand is near-absent. The in situ fragmentation of charcoal fragments is indicative of disappeared ash (Huisman et al. 2020). This unit is interpreted as hearth waste which was spread in large quantities, and possibly trampled, consistent with the maintenance considered a typical "central aisle signature" (Milek & French 2007). Higher in this unit lies a walking surface composed of a mix of decalcified ash, charcoal, and sand. Locally, zones of thinly laminated remains of organic matter (mostly amorphous or disappeared) with articulated phytoliths can be observed, while no anthropogenic inclusions save for non-metallurgical slag are present. The geochemical signal in this area is mainly rich in common anthropogenic markers such as Ba, Ca, Mg, P and Sr, and to a lesser extent also Fe. From the elemental distributions of Ca, Fe, P and Sr it appears that part of the front half of the central aisle had a possible preferred walking path crossing from one side aisle to the other, as indicated by a band with enhanced levels of these elements. Additionally, this is also reflected as low levels in Si.

This is in contrast with the southern half of Area E, represented by thin sections 16 and 17. Here, the occupation surface overlies a silty clay floor with an organic temper (A281, perhaps derived from cow or horse dung that could no longer be recognized, as attested in ethnographical research, see Lisá et al. 2020). Its localized rubification is in this case likely due to oxidation and reduction rather than in situ burning, as it is located low in the unit and contains ample iron nodules. It has been partly worn away, possibly due to traffic rather than truncation, before or while unit A263 was laid down. In this area, A263 is composed of an alternation of sand layers, decalcified ash, thin charcoal bands and thin lenses of trampled anthropogenic materials, such as bone. Both thin sections have been subjected to a relatively high amount of bioturbation, obscuring the original fabric. In thin section 17, a stronger microlamination in the top c. 1–1.5 cm points to an active floor surface with maintenance and use and an increased amount of charcoal and traces of trampling traces. In thin section 16, however, the top of the occupation surface is composed of articulated phytoliths of which the organic component has burnt in situ, representing a highly heated grass floor cover (Croix et al., 2019a; Friesem 2018).

In this part of Area E, the geochemical signal shows a depletion in most elements. Concentrations drop for Ca, Fe, Mg, P and Sr, while it remains relatively high for Si, correlating with the presence of phytoliths, molten phytoliths, sand and non-metallurgical slags identified in micromorphology. The magnetic susceptibility is increased across several smaller areas of the central aisle, possibly reflecting the presence of smaller hearths as also reflected by in situ burning and burnt clay. Fe and MS do not correlate along the central aisle.

Area F – Textile work and domestic area

This area is divided into two separate functional spaces: one in the central aisle, in the general vicinity of the hearth (A273), and one in the northwestern side aisle, interpreted as a textile working and domestic, sitting or sleeping area, possibly continuing into Area G.

The geochemical signal in Area F generally appears low in most elements, but with high concentrations of the common anthropogenic markers (Ba, K, P and Sr). Burnt clay fragments show a strong correlation to the hearth (A273), which is also visible in elevated concentrations of Ca and Sr as well as slightly lower Si-levels.

In the westernmost part of the northwestern side aisle, thin section 24 contained three subunits and was interpreted as an indoor context because of its lack of bioturbation or other disturbances, as well as the optimal preservation of anthropogenic components and articulated phytolith systems, and preferential orientation of components. However, the units were not separated during excavation. They are presumed to belong to house K22c based on their vertical position in the stratigraphy and relationship to other units of the same level. In this part, at the presumed very back of the building, a thick dump of combustion waste had been deposited. It was predominantly composed of decalcified plant ash and the remaining silica slag from phytoliths (Matthews 2010), charcoal, charred plant matter, burnt bone and clay aggregates. The paucity of sedimentary material is striking. Corresponding to this, in the western side of Area F high concentration hotspots with Cl and Na are present. These elements could originate from urine or seawater and, together with the presence of K, possibly originating from ash, and the slightly alkaline pH, this might indicate working with lye for washing or treating textiles. Alternatively, salt may have been stored in a recipient for use in e.g. food preservation in this location.

Occupation layer A263 strongly slopes down from the central aisle and hearth area towards the northwestern side aisle into what appears as a sunken-floor area. It may be due to floor collapse or a footprint in soft material, subsequently filled or repaired with ash, or it may have been established on purpose for a specific activity or for accommodating furnishing. The floor may have been less stable in this location due to the absence of a clay floor. Overall, K22c was richer in loom weight finds (27 ex.) than K23, the majority (23

ex.) being concentrated within a c. 2 × 1.5 m area in Area F (A263). The four remaining loom weights were found in Area G. Area F appears to be particularly rich in diverse domestic material, vitrified fuel ash, glass vessel sherds and glass beads, but without animal bones (Figs. 12 and 14). This might be due to the low-lying position of the area and to the softness of the deposits, making it more likely for small items to become embedded. Together with the geochemical evidence, it suggests a rather messy area, dedicated to various steps of textile processing and fabrication. Its close vicinity to the hearth area may have had practical advantages, not least in terms of comfort and light, but also a nearby source of ash for lye production.

The very back part of Area F holds low levels of almost all elements, including depleted values of Ba, which is otherwise present across the entire indoor area, except for parts of Area G. The Ba-signal resembles that of Area I, which indicates either an outdoor area or alternation with periods of indoor space here.

Area G – Sitting, sleeping, and an earlier, burnt down house area

This area is interpreted as a sitting and/or sleeping area, continuing on from and similar in use as Area F (Fig. 14). It is similar to Area F except for the position of the loom. Only a small amount of sedimentary material related to house phase K22c could be observed, as most of the thin sections contained units belonging predominantly to K22b and K23. This is also reflected in the evidence from the bulk samples, where the elevated magnetic susceptibility and general low elemental concentrations can be related to K22b.

For house phase K22c, only very little evidence is captured in the thin sections regarding this area. Only a small amount of unit A263 related to K22c was preserved, due to significant truncation and the subsequent laying down of thick, silty clay floors with an organic temper belonging to K23 (A256). The silty clay floors or preparation layers belonging to house K23 in areas G and F are extremely thick, likely to compensate for the difference in level caused by the sunken underlying layers. Based on observations from thin sections 21 and 22, an organic floor cover is likely in this area as well. However, it has become strongly bioturbated so that specific plant organs could no longer be identified, but a considerable input of organic matter has been preserved, along with some mixed-in combustion waste and clay aggregates. In the few areas where the original matrix is better preserved, a horizontal orientation of organic fragments can still be observed. Analogous to the better preserved evidence from K22b, a considerable input of grasses in the previous phase can be hypothesized. Grass stems may have served as a floor cover, or even bedding for activities such as sitting and sleeping in areas F, G, and perhaps even extending as far as Area H (see below).

Together with Area F, the size of the sitting or sleeping area would have been approximately 1.8 × 2.3 m. Perhaps this was not the only sleeping area in the house (there is no information available from the unexcavated southwestern part of the southeastern side aisle), but it would have been large enough to accommodate a number of people. Possibly, even Area H may have been included in this space.

Area H—Domestic activity in K22c makes room for metalworking in K23

In house K22c, Area H is interpreted to include domestic activities, possibly similar to those in areas F and G (Fig. 14a), while house K23 comprised a workshop for metalworking here (Fig. 14b). Both the micromorphological and geochemical results are related to house K23. Only a small portion of unit A263 belonging to K22c was captured in thin section (thin sections 19 and 20), and it appears to have been truncated, after which silty clay floor in K23, A256, was laid down. As in Area G, most of the activity surface of K22c has been removed in the building of K23 in the northwestern side aisle.

Both micromorphological samples demonstrate a moderate degree of bioturbation in unit A263, however, its original fabric can locally still be discerned. In those cases, they show an activity surface containing a mix of clay and combustion waste (mostly decalcified plant ash and charcoal) in different concentrations, as well as relatively common organic components in the form of wood chips or shavings and (semi-)continuous bands of grasses. A marked concentration of these organic components is present right beneath the clay layer (A256), where they may have been better protected from turbation. A strong horizontal orientation of elongated components suggests a gradual accumulation. Overall, the surface cover and treatment resemble that of unit A263 in the side aisle captured in areas G and F, and may suggest a similar flooring using organic bedding such as wood and bark chips or shavings and grass, as well as a similar, domestic use.

Unit A263 is truncated by a clay preparation layer or floor in the location of thin section 20, and by a thick alternation of thin clay and sand layers with abundant phosphatic and iron features, and a few traces of metalworking in thin sectione 19 (labeled unit A256 everywhere, despite its differing compositions). The pedofeatures are likely associated with elements that have moved down the stratigraphy from higher up in K23.

The geochemical signal is related to deposits from house K23 (A264). The area holds several elemental hotspots with very high concentrations of metallic elements not found elsewhere in house K22c or K23. These include

Ag, Cu, Pb, Sn and Zn, which are all known to be related to metalwork. The metal-hotspot is accompanied by the highest magnetic susceptibility values found across the analysis, probably enhanced by the increased amounts of metals in the sediment. Additionally, high concentrations of Ba, Fe, Mg and P are also found, but mainly in the northern part of the area and with corresponding low levels of Si. These common anthropogenic markers could possibly originate from a furnace or the like which was used for the metal processing. Some of the magnetic susceptibility signal would also be caused by the resulting heating. Micromorphologically, unit A264 is represented by an accumulation of distinct surfaces related to metalworking (thin section 19). Approximately twelve separate laminations could be discerned, which contained varying amounts of metal slag, metal impregnations of the fabric, traces of small mould or crucible remains, and organic remains. This area appears to have been intensively used, and an alternation between thin metalworking or dumping episodes, grass surface covers, and in situ heating of the sediment can be observed. Especially the greyish lamination in the middle of unit A264 contains abundant large metalworking slag fragments, which in microXRF imaging (Berthold & Mentzer 2017) of the impregnated block appeared to be copper. In addition, slags and impregnations of iron, copper, zinc, and lead were identified (Fig. 15), and show how different types of metals were being handled. Tin was also identified in the geochemical pXRF analysis, but not in the microXRF of the impregnated block.

Casting mould fragments are strongly associated with the floor of K23, and, apart from an overall messier area at the south end of the house, largely absent from K22c. These fragments too reflect different patterns of waste management, and the dominant craft activity performed in K23. The metallurgy workshop within K23 has a lower density of casting mould fragments, which also weigh less on average, marking the area where moulds were broken after casting and the select removal of bulky waste from the working area.

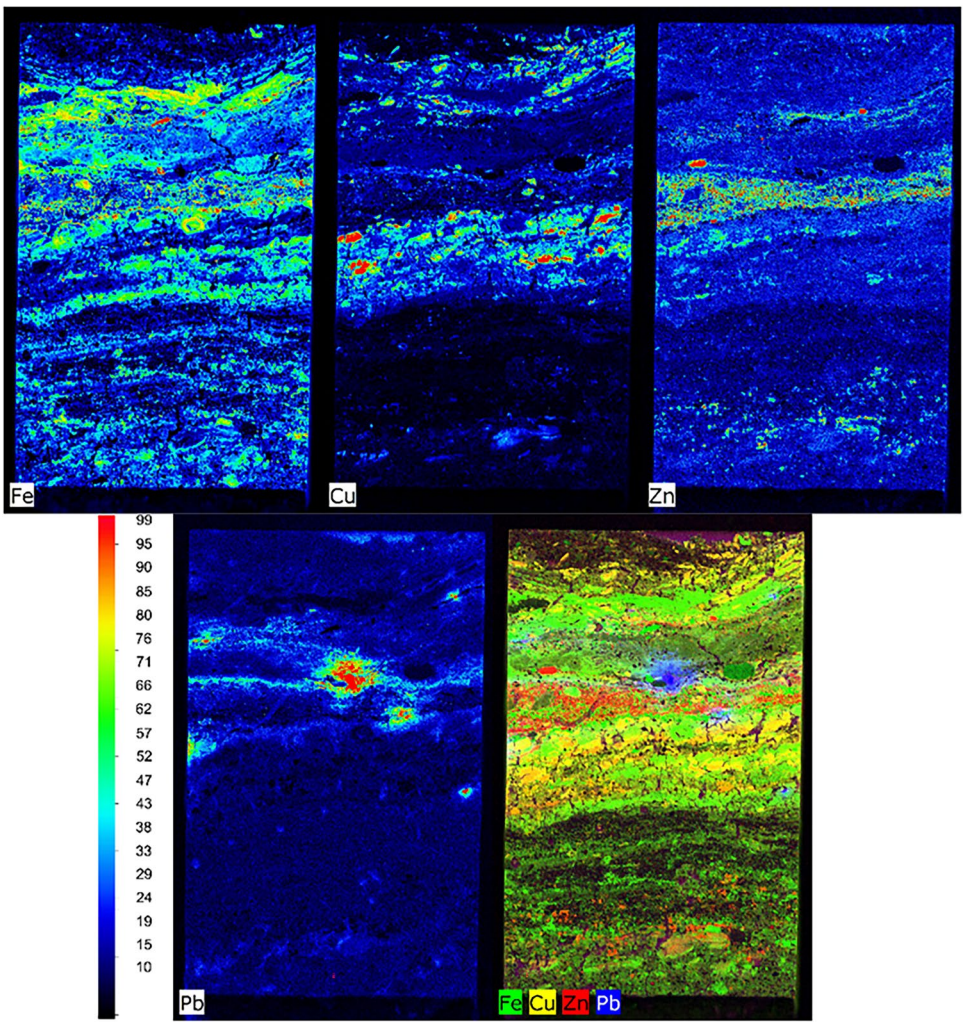

Fig. 15 MicroXRF image (resolution 25 × 25 µm) of the metalworking area captured in thin section 19 (see Fig. 11), showing the laminations of elevated Fe, Cu, Zn and Pb concentrations in ppm

Area I—Pathway

Area I is interpreted as an outdoor pathway or road (Fig. 14), consistent with the on-site interpretation. It is difficult to distinguish the precise levels that correspond to buildings K22c and K23, as there were no clear macroscopic distinctions between the stratigraphic units defined in this area. Likely, unit A291 corresponds to all phases of building K22, and units A265 and A243 correspond to building K23. The area generally appears low in most elements (Ba, Ca, Fe, K, P, Sr and As), which along with the acidic pH correlates well with leaching of the anthropogenic elements and larger minerogenic fractions as indicated by high Si concentrations. The geochemical signal clearly shows a difference between the indoor and outdoor deposits, with very low elemental concentrations in the outdoor area as defined by Area I. In the northern part of Area I, the geochemical signals approaches mean values for the depleted elements, however, they still display lower concentrations than in the indoor areas.

The micromorphological evidence shows an outdoor deposit consisting of a moderately sorted medium sized mineral fraction, with units A291 and A243 strongly resembling each other. Fluctuations in waterlogging are indicated by the presence of trace amounts of pyrite and vivianite formation (Karkanas & Goldberg 2018). These are more abundant in the lower-lying A291 corresponding to building K22c, than in A243 corresponding to K23. The lower-lying unit also contains more fine organic matter, and both contain insect remains and fungal sclerotia. The insect remains in these youngest strata on site were not preserved well enough for entomological analysis (Allison & Kenward 2022). Faunal turbation is represented by organo-mineral excremental micro-aggregates and earthworm channels. Both units contain limited anthropogenic inclusions in the form of charcoal and highly weathered, fragmented, cracked, rounded to gellified bone remains, including burnt bones, supporting the hypothesis of an outdoor context (Brönnimann et al. 2020). Most inclusions are silt to medium sand sized, with rare fragments up to 2 cm, which have a horizontal orientation but no indications for direct trampling.

All these indications lead to a hypothesis of a wooden trackway being present as, despite the wet conditions, no direct trampling, puddling, or pressing in of soil or sediment aggregates could be discerned (Banerjea et al. 2015; Rentzel et al. 2017). The low amounts of element concentrations in Area H could also support the presence of wooden planks, and hence, no predominantly sediment being deposited through the tracks, preventing a significant direct deposition of elements into the sediments below. This hypothesis is further strengthened by unit A265 which consisted of patches of mixed silt and sand at the interface between A291 and A243 in the southeastern part of Area H. The presence of molten and blackened phytoliths, as well as traces of fine charcoal, burnt bone, and non-metallurgical slag, suggest that it was originally a deposit mixed with domestic combustion waste, including ash, of which the calcitic component has been thoroughly leached. Additionally, no S appears in this unit, which contains only limited amounts of organic matter. Sulphur only appears in the outdoor areas, and especially in Area I. This element is likely correlated to the presence of organic matter, which is more pronounced in the outdoor areas than indoor. The size of the inclusions is in line with the hypothesis of a trackway. However, no microscopic traces, nor absence of wooden planks due to oxidation (cf. Gebhardt & Langohr 1999) were found, so if such planking was present, this had possibly been systematically removed during repairs. Instances of wooden trackways were encountered lower down in the stratigraphic sequence (Croix et al. 2022), thus showing precedents of this feature on site.

Area J—Household waste surrounding the building

Area J is interpreted as an open area surrounding the plot where household waste was discarded on a regular basis (Fig. 14). Generally, the micromorphological samples exhibit strong modern root and faunal turbation in Area J, especially to the southwest of the excavation area. The units captured in thin sections 8–10 can be related to the levels of houses K22 and K23, but a specific attribution to their subphases was not always possible. The clearest case for an outdoor deposit is presented by thin section 9, where the bottom unit (A343 or A291) contains evidence for the dumping of waste. This includes high amounts of amorphous organic matter, and waste related to food preparation, food consumption, and combustion, as well as traces of construction materials (clay). All bone fragments, including burnt bone, are extremely weathered or diagenised, and have suffered from bacterial and fungal attack (Fig. 10; Brönnimann et al. 2020; Huisman et al. 2017). Fungal spores, fungal sclerotia, and insect remains are present as well, and past mesofaunal bioturbation is consistent with an outdoor location (Courty et al. 1989). The different types of waste have been somewhat mixed prior to deposition, but a degree of gradual accumulation is likely, attested by the horizontal orientation of large fragments. Towards this southern part of the area, the common anthropogenic markers and plant nutrients such as Ba, Ca and P disappear from the geochemical signal and are replaced by high concentrations of K, S and acidic pH. High levels of S together with acidic pH correlate well with an increase in organic matter. Despite the absence of plant nutrients, the joint signal from micromorphological evidence and S distribution in relation to the recognized food preparation in Area C indicates likely dumping of waste into the southern part of the plot margin during the life of house K22c. In a higher-lying unit

(A291 or A243), the waste seems more strongly related to activities belonging to K23, such as a higher concentration of combustion waste rather than food preparation waste, metalworking waste specifically related to iron, and possible crucible or burnt casting mould fragments.

Thin section 8, on the contrary, is still indicative of an indoor deposit, demonstrating the extent of the roofed house into the northeastern direction. Despite high levels of bioturbation, parts of silty clay floors with an organic temper have remained preserved here (A280), at two levels. The topmost level may not be recognized as such during excavation due to its fragmentation. Both unit A288 below and A262 (possibly also A275) on top (sometimes related to outdoor deposit A266 during excavation), exhibit signs of trampling. Between the clay layers, floors appear to have consisted of strewn organic matter remains, currently no longer identifiable under the microscope, as well as spread combustion waste. Only traces of fungal spores were present in the matrix. The presence of a large bone fragment in unit A263 could be explained by its close proximity to the house wall (Banerjea et al. 2015; Macphail et al. 2004). The northern part of Area J generally shows enhanced levels of common anthropogenic markers (Ba, Ca, P and Sr) as also evident elsewhere in the indoor deposits. The pH shifts between neutral and slightly acidic here, showing the changes from indoor to outdoor deposits, but the position of this transition might be a defect from the pH-analysis only being measured in a 1.0 m grid.

For thin section 10, the evidence is less conclusive. The upper unit (attributed to A291, but perhaps in reality A262) contains decalcified ash aggregates similar to those found in thin section 8, horizontal orientation of inclusions such as organic matter, as well as traces of trampling. The charcoal is highly fragmented, suggesting a considerable past presence of ash, as in other indoor deposits. Unit A343 below it contains a gradual accumulation of food processing and/or preparation waste, including a large quantity of bone, and combustion waste. The presence of an in situ fragmented bone suggests at least one instance of trampling (Rentzel et al. 2017). However, this area does not appear to have been a ditch with standing water in the locations where it was securely interpreted as outdoor either (i.e. thin section 9), so this may not be an uncommon instance. Due to the extremely high level of bioturbation, likely enhanced by the absence of clay flooring, the micromorphological evidence is inconclusive for this unit.

Archaeological implications

Summary of interpretation

- The house floor layers investigated here show a brief, high-definition sequence of a few years in a long site history, with buildings constructed from clay, wood, wattle, bark and grasses and reeds as also described in Sindbæk (2022a).
- The sequence targeted showed mainly a phase of domestic function, including food production, as well as textile working. After a few years, the building was reconstructed and re-purposed for extensive non-ferrous metalworking.
- The house had a well-defined internal layout visible macroscopically, but its understanding is greatly improved by the geochemical analysis and soil and sediment micromorphology.
- We can trace a division into working areas answering to various practical needs in terms of light, messiness, heating. Food preparation area in C, with fire, ash, embers and food products, was kept strictly divided from a textile working area with wool and probably also plant fibres, and processes such as spinning, weaving and probably also fibre treatment with lye.
- The building was clearly a designated space for a particular range of activities. There was no trace of many other crafts practiced in the neighbourhood, and seen at other floor levels in the stratigraphy – for example iron smithing, bone and antler working, wood working, or glass bead production.
- The building shows an integration of artisanal and domestic activities under the same roof, rather than separate industrial and domestic quarters. This must reflect the social fabric of the settlement, with production characterized by domestic industries rather than separate workshop communities (cf. Ashby & Sindbæk, 2020).

Wider context in the excavation

- House phase K22c represents a period of a few years. Based on the indications from radiocarbon dates combined with the number of house phases seen in the stratigraphy, the individual sub-phase must have lasted 5–10 years on average.
- Finds from the sub-phases immediately preceding K22c suggests that a similar range of activities had characterized life in this building for some time. They include evidence for a baking oven and a loom, but few other craft-related items.
- Some 10–20 years previously, during building phase K21, the plot had been used for a bone and antler workshop, which left prolific debris. Immediately after the end of building phase K22c, a non-ferrous metal workshop was established on the plot in building K23.
- Similar shifts occur at a varying rate throughout the stratigraphy of the c. 200 year occupation history of the site. The pace of change suggests that the same occupants

may have used the building for extended periods, ranging from a few years to more than a generation.

- Most buildings examined in this early urban sequence had evidence for extensive practice of specialized crafts. In this context building K22 initially seems to stand somewhat apart, with its mainly "domestic" activities of food production and textile working. Evidence for textile work is present in most buildings examined in the town, and appears to have been a widespread household industry. In early medieval Scandinavia, textile working was generally considered a female domain, and the widespread textile working may thus indicate that the houses were often home to family units, rather than, for example, itinerant craftspeople or servile labourers.
- This is consistent with evidence from the town's cemetery, which shows graves of women, men and children (Croix 2020b).
- However, the presence of the baking oven may indicate that the occupants of building K22c also had a special trade. Remains of ovens are only found in a few of the many buildings examined in the site. This could suggest that bread and other food was prepared here for a wider neighbourhood. While not a craft for wider circulation like comb-making or glass bead production, this form of production and its practitioners would have been a significant part of the internal economic networks of the early urban community.

'Experimental' elements; hypotheses and questions for further research

Arsenic and manganese concentrations were only elevated in the food preparation part of Area C. Since the elements are only distributed in this limited area with known use, it appears to be a marker for food processing or foodstuffs in general. Arsenic can in aerobic environments be associated with organic matter (Alloway 2013), which is probably why it appears as a marker in this area. However, future studies are needed to further clarify this relationship, especially for As, in archaeological contexts outside metalworking areas.

In the back part of the house, Area F holds one large hotspot with coinciding high concentrations of both Cl and Na. The combination of these two elements is usually related to presence of seawater or urine (Milek & Roberts 2013; Sulas et al. 2017). In this study, the two elements are present together with large amounts of ashes and alkaline pH, possibly indicating the use of urine or seawater for production of lye for textile working. However, the high-concentration areas of Cl and Na are closely located to the possible place of a weaving loom, so perhaps it was simply an area used for the storage of lye or soap (e.g. in a barrel) rather than the in situ processing or cleaning of wool.

An apparent difference between indoor and outdoor deposits seems in Ribe to be indicated by the presence of S, as enhanced concentrations were only found in the outdoor deposits related to the pathway in front and plot margin east of the house. However, since S bonds strongly to organic matter and can be found in plant material (Bohn et al. 2001; Cannell et al. 2020), the relationship is probably between organic rich deposits and S instead of indoor/outdoor areas. This is supported by Cannell et al. (2020) who associated S to either organic matter, pyrite (FeS_2) or argentite (Ag_2S). Here, only trace amounts of pyrite were observed during micromorphological analysis, and no enhanced levels of Ag or Fe are found related to S. Hence, it is most likely that organic matter is the source of S. Indoor deposits from Ribe did contain some organic matter, but in these excavation units it was completely decomposed so that only silica bodies remain, and hence, one possibility is that S-concentrations are linked to the preservation state of the organic matter. We encourage future studies to include further analysis on the relationship between S and organic matter in archaeological and anthropological studies.

Finally, we found that Si appears to be a useful marker for chemically "clean" indoor areas (e.g. in Area E), since the weight percentage of Si will be relatively higher when other elements are not deposited or retained in a natural sediment. As noted by Cannell et al. (2020), Si is usually inherited from coarser silicate minerals, quartz and clays, and it can as such also be included as a marker for the geological input to the deposits. Additionally, inorganic residues of biological origin, such as phytoliths and diatoms, could also enhance the amounts of Si measured. Regardless of its origin being mainly geological, Si appears useful as an archaeological proxy when other elements are missing or low due to e.g. cleaning as suggested here.

Conclusion

This paper demonstrates how a combined approach of micromorphology, geochemistry and the study of artefact distributions presents a good fit to characterise and map the activities and use of space of a building's indoor and outdoor setting. In addition, the contribution of micromorphology in particular, is to enhance our understanding of the complex stratigraphy and depositional history of an urban site as a framework for the artefactual and geochemical evidence. It confirms the result of ethnographical studies, namely that truncations and house maintenance are an important part of the archaeological record, and often remain better visible than some of the anthropogenic activities that took place. Geochemistry, on the other hand, is better suited to demarcate larger areas of use, since

the number of samples that can be analysed provides an increased coverage of the surface.

Some parts of the house analysed for this study at the Viking-Age emporium Ribe did not contain clay floors, causing problems with the distinction between the two house phases under scrutiny, K22c and K23. Locally, the breaking and sinking of floors showed continued issues with structural stability. Nevertheless, a division into areas where specific activities took place could be proposed for house K22c (c. 790–810). The house served a predominantly domestic purpose, as opposed to earlier and younger phases, where respectively glass bead making and metalworking are attested. The central aisle was the main area of traffic, while the side aisles and front rooms housed activities such as food processing, sitting or sleeping, weaving, and storage. On the basis of these functional areas, it can be hypothesised that the front part of the house was a place for social contact with the urban community, while the domestic life of the household was centred around the hearth at the back. A shift in activities was apparent between house K22c and younger K23, where the northwestern aisle shifted from being used for sitting or sleeping to metalworking, and the southeastern side aisle from the processing of food to weaving and possibly sitting area.

Finally, we suggest a number of "new" elements that show interpretative potential, which are advised to be included in future research. Arsenic and Mn were only visible in the food preparation area of the house, and hence appears to be markers for activities related to food processing or foodstuffs in general. Near the location of a weaving loom in Area F and G, concentrations were high for Cl and Na, possibly indicating storage for lye or soap, which could be used in combination with production of textiles using lye. Sulphur appears to reflect deposits rich in organic matter, possibly depending on the preservation state of the organic matter, since no S was recognized in indoor deposits where all organic matter was oxidised. Lastly, usability of Si and S in archaeological contexts warrants further attention, i.e. to reflect areas that have been kept clean and areas high in decomposed organic matter. A multi-proxy geochemical and micromorphological study is made for complexity. In using the result to make sense of the use of space and stratigraphy, simplicity is indeed a virtue; but it certainly requires hard work to achieve it.

Abbreviations A[number]: Stratigraphic units and its excavation ID number (e.g., A264); FL: Fluorescent light microscopy; K[number]: House construction phase and its excavation ID number (e.g., K23); µXRF: Micro-X-ray fluorescence; MS: Magnetic susceptibility; OIL: Oblique incident light; OM: Organic matter; PPL: Plane-polarized light (PPL); pXRF: Portable-X-ray fluorescence; SOM: Soil organic matter; XPL: Crossed polarizers (XPL)

Acknowledgements The authors would like to thank everyone on the Northern Emporium excavation team and the Museum of Southwest Jutland.

Author Contributions Conceptualization: B.W. and P.L.K.T. Data curation: B.W.and P.L.K.T. Formal analysis: B.W. and P.L.K.T. Funding acquisition: S.M.S. Investigation: B.W., P.L.K.T, S.C., S.M.S., P.D., S.M.K. Methodology: B.W., P.L.K.T, S.C., S.M.K. Project administration: S.M.S. Resources: S.M.S. Visualization: B.W., P.L.K.T, P.D., S.C. Writing – original draft: B.W., P.L.K.T. Writing – review & editing: B.W., P.L.K.T, S.C., S.M.S., P.D., S.M.K.

Funding Open access funding provided by Aarhus Universitet. The excavation and the Northern Emporium Project were funded by a Semper Ardens grant from the Carlsberg Foundation. This work was supported by the Danish National Research Foundation under the grant DNRF119—Centre of Excellence for Urban Network Evolutions (UrbNet), and a postdoctoral research fellowship (12S7318N) of the Research Foundation Flanders – FWO. The authors would like to express their gratitude to the funders, as well as their respective institutions for supporting their work. The funders had no role in study design, data collection and analysis, decision to publish, or preparation of the manuscript.

Data availability All relevant data are within the manuscript and in the Supporting Information section.

Declarations

Competing interests The authors declare no competing interests.

References

Allison E, Kenward H (2022) Insect remains from excavations at Posthustorvet in Ribe. In: S. M. Sindbæk (Ed.), *Northern Emporium vol. 1: The Making of Viking-age Ribe* (pp. 389–416). Højbjerg: Jutland Archaeological Society, 389–416

Alloway BJ (2013) Heavy Metals in Soils: Trace Metals and Metalloids in Soils and their Bioavailability. Springer

Arpin TL, Mallol C, Goldberg P (2002) A new method of analyzing and documenting micromorphological thin sections using flatbed scanners: Applications in geoarchaeological studies. Geoarchaeology 17:305–313

Ashby S, Sindbæk SM (2020) Between domestic circles and urban networks. In: Ashby S, Sindbæk SM (eds) Crafts and Social Networks in Viking Towns. Oxbow, Oxford, pp 53–58

Ashby SP, Coutu AN, Sindbæk SM (2015) Urban Networks and Arctic Outlands: Craft Specialists and Reindeer Antler in Viking Towns. Eur J Archaeol 18(4):679–704. https://doi.org/10.1179/1461957115y.0000000003

Banerjea RY, Bell M, Matthews W, Brown AD (2015) Applications of micromorphology to understanding activity areas and site formation processes in experimental hut floors. Archaeol Anthropol Sci 7:89–112

Banerjea RY (2018) The micromorphology of refuse disposal and the use of the earliest features of in Insula IX. In: M. Fulford, A. Clarke, E. Durham, & N. Pankhurst (Eds.), *Late Iron Age Calleva: The Pre-Conquest Occupation At Silchester Insula IX* (pp. 358–370). Promotion for Roman Studies. Britannia Monograph Series 32

Barfod GH, Feveile C, Sindbæk SM (2022) Splinters to splendours: from upcycled glass to Viking beads at Ribe, Denmark. Archaeol Anthropol Sci 14(9):180. https://doi.org/10.1007/s12520-022-01646-8

Barrett JH, Hall A, Johnstone C, HK, O'Connor TSA (2007) Interpreting the Plant and Animal Remains from Viking-age Kaupang. In: D. Skre (Ed.), *Kaupang in Skiringssal. Kaupang Excavation Project Publication Series* 1, pp 283–319. Aarhus University Press, Aarhus

Bencard M, Jørgensen LB (1990) Excavation and stratigraphy. In: Bencard M, Jørgensen LB, Madsen HB (eds) Ribe excavations 1970–1976, 4. Sydjysk Universitetsforlag, Esbjerg, pp 15–163

Benyarku CA, Stoops G (2005) No Guidelines for preparation of rock and soil thin sections and polished sections. In U. de Lleida (Ed.), *Quaderns DMACS 33*. Lleida

Bern CR (2009) Soil chemistry in lithologically diverse datasets: The quartz dilution effect. Appl Geochem 24(8):1429–1437. https://doi.org/10.1016/j.apgeochem.2009.04.013

Berthold C, Mentzer SM (2017) X-ray microdiffraction. In: Nicosia C, Stoops G (eds) Archaeological Soil and Sediment Micromorphology. Wiley Blackwell, Oxford, pp 417–429

Blume H-P, Brümmer GW, Fleige H, Horn R, Kandeler E, Kögel-Knabner I, Wilke B-M (2015) *Scheffer/Schachtschabel Soil Science*. Springer Nature

Bohn HL, McNeal BI, O'Connor GA (2001) Soil geochemistry. John Wiley & Sons Inc

Borderie Q, Ball T, Banerjea R, Bizri M, Lejault C, Save S, Vaughan-Williams A (2020) Early Middle Ages Houses of Gien (France) from the Inside: Geoarchaeology and Archaeobotany of 9th–11th c. Floors Environ Archaeol 25:151–169

Breuning-Madsen H, Holst M, Rasmussen M (2001) The chemical environment in a barrow shortly after construction – an archaeological-pedological experiment. J Archaeol Sci 29:691–697

Brönnimann D, Wimmer J, Müller-Kissing M, Stopp B, Rissanen H, Spichtig N (2020) One man's trash is another man's treasure. Interdisciplinary examination of taphonomic aspects of ceramic sherds, animal bones and sediments from the La Tène period settlement at Basel-Gasfabrik. PLoS ONE 15(7):e0236272. https://doi.org/10.1371/journal.pone.0236272

Cannell RJS, Bill J, Cheetham P, Welham K (2020) Geochemical analysis of the truncated Viking Age trading settlement of Heimdalsjordet, Norway. Geoarchaeology 35:1–24. https://doi.org/10.1002/gea.21795

Canti MG, Brochier JE (2017) Plant ash. In: Nicosia C, Stoops G (eds) Archaeological Soil and Sediment Micromorphology. Wiley Blackwell, Oxford, pp 147–154

Cook SR, Clarke AS, Fulford MG, Voss J (2014) Characterising the use of urban space: A geochemical case study from Calleva Atrebatum (Silchester, Hampshire, UK) Insula IX during the late first/early second century AD. J Archaeol Sci 50(1):108–116. https://doi.org/10.1016/j.jas.2014.07.003

Courty MA (2001) Microfacies Analysis Assisting Archaeological Stratigraphy. In: Goldberg P, Holliday VT, Ferring CR (eds) Earth Sciences and Archaeology. Springer, Boston, MA, pp 205–239

Courty M-A, Goldberg P, Macphail RI (1989) Soils and Micromorphology in Archaeology. Cambridge University Press, Cambridge

Crabtree PJ, Reilly E, Wouters B, Devos Y, Bellens T, Schryvers A (2017) Environmental evidence from early urban Antwerp: New data from archaeology, micromorphology, macrofauna and insect remains. Quatern Int 460:108–123. https://doi.org/10.1016/j.quaint.2017.08.059

Crabtree PJ (2018) Early medieval Britain. The rebirth of towns in the post-Roman West. Cambridge University Press

Croix S (2015) Permanency in Early Medieval Emporia: Reassessing Ribe. Eur J Archaeol 18(3):497–523. https://doi.org/10.1179/1461957114y.0000000078

Croix S (2020a) Objects, Contexts, and Use of Space: The 'Biography' of a Workshop in Eighth-Century Ribe. J Urban Archaeol 2:15–30. https://doi.org/10.1484/J.JUA.5.121526

Croix S (2020b) Ribe's Pre-Christian cemetery: The Burial customs of an Early Urban Community. In: A. Pedersen & S. M. Sindbæk (Eds.), *Viking Encounters. Proceedings of the Eighteenth Viking Congress*. Aarhus University Press

Croix S, Deckers P, Feveile C, Knudsen M, Qvistgaard SS, Sindbæk SM, Wouters B (2019a) Single Context, Metacontext, and High Definition Archaeology: Integrating New Standards of Stratigraphic Excavation and Recording. *Journal of Archaeol Method Theory*. pp 465–480. https://doi.org/10.1007/s10816-019-09417-x

Croix S, Neiβ M, Sindbæk SM (2019b) The réseau opératoire of Urbanization: Craft Collaborations and Organization in an Early Medieval Workshop in Ribe. Denmark Cambridge Archaeological Journal 29(2):345–364. https://doi.org/10.1017/S0959774318000525

Croix S, Deckers P, Feveile C, Knudsen M, Qvistgaard SS, Sindbæk SM, Wouters B (2022) Excavation atlas. In: S. M. Sindbæk (Ed.), *Northern Emporium vol. 1: The Making of Viking-age Ribe*. Højbjerg: Jutland Archaeological Society. pp 49-217

Deckers P (2022) Site formation and artefact assemblages. In: S. M. Sindbæk (Ed.), *Northern Emporium vol. 1: The Making of Viking-age Ribe*. Højbjerg: Jutland Archaeological Society. pp 217-300.

Devos Y (2018) Near total and inorganic phosphorus concentrations as a proxy for identifying ancient activities in urban contexts: The example of dark earth in Brussels, Belgium. Geoarchaeology 33:470–485

Devos Y, Nicosia C, Wouters B (2020) Urban Geoarchaeology in Belgium: Experiences and innovations. Geoarchaeology 35(1):27–41

Dore CD, Varela SLL (2010) Kaleidoscopes, palimpsests, and clay: Realities and complexities in human activities and soil chemical/residue analysis. J Archaeol Method Theory 17(3):279–302. https://doi.org/10.1007/s10816-010-9092-x

Entwistle JA, Abrahams PW (1997) Multi-Element Analysis of Soils and Sediments from Scottish Historical Sites. The Potential of Inductively Coupled Plasma-Mass Spectrometry for Rapid Site Investigation. J Archaeol Sci 24:407–416

F.A.O. (2006) Guidelines for soil description, 4th edition. Rome: Food and Agriculture Organization of the United Nations

Feveile, C. & Sindbæk, S. M. (2022). The excavation at SJM 3 Posthustorvet. In: S. M. Sindbæk (Ed.), *Northern Emporium vol. 1: The Making of Viking-age Ribe*. Højbjerg: Jutland Archaeological Society, 25–48. pp 25–48

Feveile C, Jensen S (2000) Ribe in the 8th and 9th century: A contribution to the archaeological chronology of north western Europe. Acta Archaeologica 71(1–2):9–24. https://doi.org/10.1034/j.1600-0390.2000.d01-2.x

Feveile C (2006a) Ribe On the North Side of the River, 8th–12th Century——Overview and Interpretation. In Claus Feveile (Ed.), *Ribe Studier. Det Ældste Ribe. Udgravninger på nordsiden af Ribe Å 1984–2000. Bind 1.1*. Jysk Arkæologisk Selskab. pp 65–91

Feveile C (2006b) *Ribe studier: Det ældste Ribe. Udgravninger på nordsiden af Ribe Å 1984–2000,* (C. Feveile, Ed.). Højbjerg: Jysk Arkæologisk Selskab, *1.1–1.2*

Feveile C (2012) Ribe: Emporia and Town in 8th–9th Century. In S. Gelichi & R. Hodges (Eds.), *From One Sea to Another. Trading*

Places in the European and Mediterranean Early Middle Ages. Proceedings of the International Conference Comacchio, 27–29 March 2009 (pp. 111–122). Brepols Publishers

Fleisher J, Sulas F (2015) Deciphering public spaces in urban contexts: Geophysical survey, multi-element soil analysis, and artifact distributions at the 15th-16th-century AD Swahili settlement of Songo Mnara, Tanzania. J Archaeol Sci 55:55–70. https://doi.org/10.1016/j.jas.2014.12.020

Friesem D (2018) Geo-ethnoarchaeology of Fire: Geoarchaeological Investigation of Fire Residues in Contemporary Context and its Archaeological Implications. Ethnoarchaeology 10:159–173

Gebhardt A, Langohr R (1999) Micromorphological study of construction materials and living floors in the medieval motte of Werken (West Flanders, Belgium). Geoarchaeology 14:595–620

Goldberg P, Macphail RI (2006) Practical and Theoretical Geoarchaeology. Blackwell, Oxford

Grabowski R, Linderholm J (2014) Functional interpretation of Iron Age longhouses at Gedved Vest, East Jutland, Denmark: multiproxy analysis of house functionality as a way of evaluating carbonised botanical assemblages. Archaeol Anthropol Sci 6:329–343. https://doi.org/10.1007/s12520-013-0161-4

Heimdahl J (2005) Urbanised nature in the past: Site formation and environmental development in two Swedish towns, AD 1200–1800. Stockholm University, Stockholm

Huisman DJ, Ismail-Meyer K, Sageidet BM, Joosten I (2017) Micromorphological indicators for degradation processes in archaeological bone from temperate European wetland sites. J Archaeol Sci 85:13–29

Huisman DJ, Braadbaart F, van Wijk I, Van Os BJH (2020) Ashes to ashes, charcoal to dust: Micromorphological evidence for ash-induced disintegration of charcoal in Early Neolithic (LBK) soil features in Elsloo (The Netherlands). J Archaeol Sci 39:994–1004

Ismail-Meyer K, Stolt M, Lindbo D (2018) Soil organic matter. In: G. Stoops, V. Marcelino, & F. Mees (Eds.), *Interpretation of Micromorphological Features of Soils and Regoliths* (2nd ed.,). Elsevier, Amsterdam. Pp 471–512

Karkanas P, Goldberg P (2018) Phospatic features. In: Stoops G, Marcelino V, Mees F (eds) Interpretation of micromorphological features of soils and regoliths, 2nd edn. Elsevier, Amsterdam, pp 323–246

Karkanas P, Van de Moortele A (2014) Micromorphological analysis of sediments at the Bronze Age site of Mitrou, central Greece: patterns of floor construction and maintenance. J Archaeol Sci 43:198–213

Kooistra MJ, Pulleman MM (2018) Features related to faunal activity. In: G. Stoops, V. Marcelino, & F. Mees (Eds.), *Interpretation of Micromorphological Features of Soils and Regoliths*. Elsevier, Amsterdam. 2nd ed., pp 447–469

Kristiansen SM, Tjelldén AKE (2022) The Emporium' In-situ preservation conditions: geoarchaeological evidence and environmental monitoring recommendations. In: Sindbæk SM (ed) Northern Emporium, vol 1. The. Jutland Archaeological Society, Højbjerg, pp 315–326

Langohr, R. (1994). Directives and rationale for adequate and comprehensive field soil data bases. In *New waves in soil science. Refresher course for alumni of the international training centre for post-graduate soil scientists of the Ghent University, Harare* (pp. 176–191). Gent: International Training Centre University Ghent.

Linderholm, J., & Lundberg, E. (1994). Chemical Characterization of Various Archaeological Soil Samples using Main and Trace Elements determined by Inductively Coupled Plasma Atomic Emission Spectrometry. *Journal of Archaeological Science*, *21*, 303–314. https://doi.org/10.1006/jasc.1994.1030

Lisá L, Kočár P, Bajer A, Kočárová R, Syrová Z, Syrový J, Ježková M (2020) The floor: a voice of human lifeways—a geo-ethnographical study of historical and recent floors at Dolní Němčí Mill Czech Republic. Archaeol Anthropol Sci 12:115. https://doi.org/10.1007/s12520-020-01060-y

Loveluck C (2013) Northwest Europe in the early Middle Ages, c. AD 600–1150: A comparative archaeology. Cambridge: Cambridge University Press

Macphail RI, Goldberg P (2017) Applied Soils and Micromorphology in Archaeology. Cambridge University Press, Cambridge

Macphail RI, Cruise GM, Allen MJ, Linderholm J, Reynolds P (2004) Archaeological soil and pollen analysis of experimental floor deposits; with special reference to Butser Ancient Farm, Hampshire. UK Journal of Archaeological Science 31(2):175–191

Macphail RI, Bill J, Crowther J, Haită CJ, Popovici D, Rødsrud CL (2016) European ancient settlements – A guide to their composition and morphology based on soil micromorphology and associated geoarchaeological techniques; introducing the contrasting sites of Chalcolithic Borduşani-Popină. Quaternary International, Borcea River, Romania and Viking Age. https://doi.org/10.1016/j.quaint.2016.08.049

Malbos L (2017) Les ports des mers nordiques à l'époque viking (VIIe–Xe siècle). Brepols Publishers, Turnhout

Mallol C, Mentzer SM (2017) Contacts under the lens: Perspectives on the role of microstratigraphy in archaeological research. Archaeol Anthropol Sci 9:1645–1669

Matthews W (2010) Geoarchaeology and taphonomy of plant remains and microarchaeological residues in early urban environments in the Ancient Near East. Quatern Int 214(1–2):98–113

Matthews W, French CAI, Lawrence T, Cutler DF, Jones MK (1997) Microstratigraphic traces of site formation processes and human activities. World Archaeol 29(2):281–308

Matthews W (2005) Micromorphological and microstratigraphic traces of uses and concepts of space. In: I. Hodder (Ed.), *Inhabiting Çatalhöyük: reports from the 1995–99 seasons/by members of the Çatalhöyük teams*. McDonald Institute for Archaeological Research, Cambridge; British Institute of Archaeology at Ankara, London

Mikołajczyk Ł, Milek K (2016) Geostatistical approach to spatial, multi-elemental dataset from an archaeological site in Vatnsfjörður, Iceland. J Archaeol Sci Rep 9:577–585. https://doi.org/10.1016/j.jasrep.2016.08.036

Milek KB (2005) Soil Micromorphology. In: Sharples N (ed) A Norse Farmstead in the Outer Hebrides, Excavation at Mound 3, Bornais, South Uist. Oxbow, Oxford, pp 35–36

Milek KB (2012) Floor formation processes and the interpretation of site activity areas: An ethnoarchaeological study of turf buildings at Thverá, northeast Iceland. J Anthropol Archaeol 31(2):119–137. https://doi.org/10.1016/j.jaa.2011.11.001

Milek K, French C (2007) Soils and Sediments in the Settlement and Harbour at Kaupang. In: Skre D (ed) Kaupang in Skiringssal, Kaupang Excavation Project Publication Series. Aarhus University Press, Aarhus, pp 321–360

Milek KB, Roberts HM (2013) Integrated geoarchaeological methods for the determination of site activity areas: A study of a Viking Age house in Reykjavik. Iceland Journal of Archaeological Science 40(4):1845–1865. https://doi.org/10.1016/j.jas.2012.10.031

Milek K, Zori D, Connors C, Baier W, Baker K, Byock J (2014) Interpreting social space and social status in the Viking Age house at Hrísbrú using integrated geoarchaeological and microrefuse analyses. In: D. Zori & J. Byock (Eds.), *Viking Archaeology in Iceland: The Mosfell Archaeological Project* pp143–162. https://doi.org/10.1484/M.CURSOR-EB.1.102218

Naylor J (2016) Emporia and Their Hinterlands in the 7th to 9th Centuries AD: Some Comments and Observations from England. In: I. Leroy & L. Verslype (Eds.), *Les cultures des littoraux au haut Moyen Âge. Cadres et modes de vie dans l'espace maritime Manche-mer du Nord du IIIe au Xe s.*. Villeneuve d'Ascq: Revue Du Nord. pp 59–67

Nielsen NH, Kristiansen SM (2014) Identifying ancient manuring: traditional phosphate vs. multi-element analysis of archaeological soil. J Archaeol Sci 42:390–398. https://doi.org/10.1016/j.jas.2013.11.013

Oonk S, Slomp CP, Huisman DJ, Vriend SP (2009) Effects of site lithology on geochemical signatures of human occupation in archaeological house plans in the Netherlands. J Archaeol Sci 36(6):1215–1228. https://doi.org/10.1016/j.jas.2009.01.010

Orfanou, V., Birch, T., Sindbæk, S. M., Feveile, C., Barfod, G. H., & Lesher, C. (2021). On diverse arts: crucible metallurgy and the polymetallic cycle at Scandinavia's earliest Viking town, Ribe (8th–9th c. CE), Denmark. *Archaeological and Anthropological Sciences*, *13*(5), [81]. https://doi.org/10.1007/s12520-021-01308-1

Parker RB, Toots H (1970) Minor Elements in Fossil Bone. Geol Soc Am Bullet 81(3):925–932. https://doi.org/10.1130/0016-7606(1970)81[925:MEIFB]2.0.CO;2

Philippsen B, Feveile C, Olsen J, Sindbæk SM (2022) Single-year radiocarbon dating anchors Viking Age trade cycles in time. Nature 601(7893):392–396. https://doi.org/10.1038/s41586-021-04240-5

Rentzel P, Nicosia C, Gebhardt A, Brönnimann D, Pümpin C, Ismail-Meyer K (2017) Trampling, Poaching and the Effect of Traffic. In: Nicosia C, Stoops G (eds) Archaeological Soil and Sediment Micromorphology. Wiley & Sons, Oxford, pp 281–297

Rondelli B, Lancelotti C, Madella M, Pecci A, Balbo A, Pérez JR, Ajithprasad P (2014) Anthropic activity markers and spatial variability: An ethnoarchaeological experiment in a domestic unit of Northern Gujarat (India). J Archaeol Sci 41:482–492. https://doi.org/10.1016/j.jas.2013.09.008

Schulin R, Jonhnson A, Frossard E (2010) Trace element-deficient soils. In: Hooda PS (ed) Trace Elements in soils. Wiley, pp 175–198

Shahack-Gross R, Albert RM, Gilboa A, Nagar-Hillman O, Sharon I, Weiner S (2005) Geoarchaeology in an urban context: the uses ofspace in a Phoenician monumental building at Tel Dor (Israel). J Archaeol Sci 32:1417–1431

Shillito L-M (2013) Surfaces and streets: phytoliths, micromorphology and changing use of space at Neolithic Çatalhöyük (Turkey). Antiquity 87(337):684–700

Shillito L-M (2017) Multivocality and multiproxy approaches to the use of space: lessons from 25 years of research at Çatalhöyük. World Archaeol 49(2):237–259

Sindbæk SM (2018) Northern Emporium: The archaeology of urban networks in Viking-Age Ribe. In: Raja R, Sindbæk SM (eds) Urban Network Evolutions: Towards a high-definition archaeology. Aarhus, Aarhus University Press, pp 161–166

Sindbæk, S. M., & Athena Trakadas. (2014). *The World in the Viking Age* (S. M. Sindbæk & A. Trakadas, Eds.). The Viking Ship Museum.

Sindbæk SM (2015) Northern emporia and maritime networks. Modelling past communication using archaeological network analysis. In J. Preiser-Kapeller & F. Daim (Eds.), *Harbours and Maritime Networks as Complex Adaptive Systems*. Mainz: Verlag des Römisch-Germanischen Zentralmuseums. pp 1105–1117

Sindbæk SM (Ed.) (2022a) Northern Emporium vol. 1: The Making of Viking-age Ribe. Højbjerg: Jutland Archaeological Society.

Sindbæk, S. M. (2022b). Emporia, high-definition archaeology, and Ribe. In S. M. Sindbæk (Ed.), *Northern Emporium vol. 1: The Making of Viking-age Ribe* (pp. 11–23). Højbjerg, Jutland Archaeological Society.

Skre, D. (2008). Post-substantivist Towns and Trade AD 600–1000. In: D. Skre, (Ed)., *The Means of Exchange. Kaupang Excavation Project Publication Series, Vol. 2*. Aarhus: Aarhus University Press, 327–341.

Skre, D. (2011). The Inhabitants: Activities. In D. Skre (Ed.), *Things from the Town. Artefacts and Inhabitants in Viking-Age Kaupang. Kaupang Excavation Project Publication Series, Vol. 3* (Vol. 3). Aarhus University Press, Aarhus.

Smith H, Marshall P, Pearson MP (2001) Reconstructing House Activity Areas. In: U. Albarella (Ed.), *Environmental Archaeology: Meaning and Purpose* pp 249–270. https://doi.org/10.1007/978-94-015-9652-7

Sode T, Feveile C, Schnell U (2010) An investigation on segmented, metal-foiled glass beads and blown, mirrored glass beads from Ribe, Denmark. In J. Callmer, C. Theune, F. Biermann, R. Struwe, & G. H. Jeute (Eds.), *Zwischen Fjorden und Steppe: Festschrift für Johan Callmer zum 65. Geburtstag*. Verlag Marie Leidorf: Rahden/Westf. pp 319–328

Sode T, Feveile C (2002) Segmenterede metalfolierede flasperler og blæste hule glasperler med metalbelægning fra markedspladsen i Ribe. In: Kieffer-Olsen J, Benthien S, Feveile C, Hammer L, Melbye KM, Mulvad S, Skønager L (eds) By, marsk og geest 14. Forlaget Liljebjerget, pp 5–12

Søvsø M (2020) Ribe 700–1050. From Emporium to Civitas in Southern Scandinavia. Højbjerg: Jutland Archaeological Society.

Stoops G (2003) Guidelines for analysis and description of soil and regolith thin sections (3rd editio). Soil Science Society of America

Sulas F, Fleisher J, Wynne-Jones S (2017) Geoarchaeology of urban space in tropical island environments: Songo Mnara, Tanzania. J Archaeol Sci 77:52–63. https://doi.org/10.1016/j.jas.2016.06.002

Sulas F, Kristiansen SM, Wynne-Jones S (2019) Soil geochemistry, phytoliths and artefacts from an early Swahili daub house Unguja Ukuu Zanzibar. J Archaeol Sci 103(May 2018):32–45. https://doi.org/10.1016/j.jas.2019.01.010

Trant PLK, Kristiansen SM, Sindbæk SM (2020) Visible near-infrared spectroscopy as an aid for archaeological interpretation. Archaeol Anthropol Sci 12:280. https://doi.org/10.1007/s12520-020-01239-3

Trant PLK, Kristiansen SM, Christiansen AV, Wouters B, Sindbæk SM (2021) Sampling density and spatial analysis: a methodological pXRF study of the geochemistry of a Viking-Age house in Ribe, Denmark. Archaeol Anthropol Sci 13(1):21. https://doi.org/10.1007/s12520-020-01243-7

Tyler G (2004) Vertical distribution of major, minor, and rare elements in a Haplic Podzol. Geoderma 119(3):277–290. https://doi.org/10.1016/j.geoderma.2003.08.005

Tys D (2020) Maritime and River Traders, Landing Places, and Emporia Ports in the Merovingian Period in and Around the Low Countries. In: Effros B, Moreira I (eds) The Oxford Handbook of the Merovingian World. Oxford, Oxford University Press, pp 765–798

Vepraskas MJ, Lindbo DL, Stolt MH (2018) Redoximorphic features. In: Stoops G, Marcelino V, Mees F (eds) Interpretation of micromorphological features of soils and regoliths, 2nd edn. Elsevier, Amsterdam, pp 425–445

Wilson CA, Davidson DA, Cresser MS (2005) An evaluation of multielement analysis of historic soil contamination to differentiate space use and former function in and around abandones farms. The Holocene 15(7):1094–1099. https://doi.org/10.1191/0959683605hl881rr

Wilson CA, Davidson DA, Cresser MS (2008) Multi-element soil analysis: an assessment of its potential as an aid to archaeological interpretation. J Archaeol Sci 35:412–424. https://doi.org/10.1016/j.jas.2007.04.006

Woodruff LG, Cannon WF, Eberl DD, Smith DB, Kilburn JE, Horton JD, Klassen RA (2009) Continental-scale patterns in soil geochemistry and mineralogy: Results from two transects across the United States and Canada. Appl Geochem 24(8):1369–1381. https://doi.org/10.1016/j.apgeochem.2009.04.009

Wouters B, Makarona C, Nys K, Claeys P (2017) Characterization of Archaeological Metal Remains in Micromorphological Thin Sections Using μXRF Elemental Mapping. Geoarchaeology 32(2):311–318. https://doi.org/10.1002/gea.21591

Wouters B, Milek K, Devos Y, Tys D (2016) Micromorphology in urban research: Early medieval Antwerp (Belgium) and Viking Age Kaupang (Norway). In B. Jervis, L. Broderick, & I. G. Sologestoa (Eds.), *Objects, Environment, and Everyday Life in Medieval Europe*. Turnhout: Brepols. pp 279–295

Wouters B (2018) Geoarchaeology and micromorphology at Ribe: A Northern Emporium in high definition. In Rubina Raja & S. M. Sindbæk (Eds.), *Urban Network Evolutions. Towards a high-definition archaeology*. Aarhus University Press. pp 175–182

Wouters B (2022) Soil and sediment micromorphology. In S. M. Sindbæk (Ed.), *Northern Emporium: Vol. 1 The Making of Viking-age Ribe*. Højbjerg, Jutland Archaeological Society. 1, pp 239–270

Zak D, Hupfer M, Cabezas A, Jurasinski G, Audet J, Kleeberg A, Mcinnes R, Kristiansen SM, Liu H, Petersen JR, Goldhammer T (2021) Sulphate in freshwater ecosystems: A review of sources, biogeochemical cycles, ecotoxicological effects and bioremediation. Earth Sci Rev 212:103446. https://doi.org/10.1016/j.earscirev.2020.103446